# The new synthetic and runs-rules schemes to monitor the process mean of autocorrelated observations with measurement errors *

Sandile Charles Shongwe, Jean-Claude Malela-Majika, Philippe Castagliola

# The new synthetic and runs-rules schemes to monitor the process mean of autocorrelated observations with measurement errors

*Shongwe S.C.[1], Malela-Majika J.-C.[1], Castagliola P.[2]

**Abstract**

The use of the 2-*of*-(*H*+1) runs-rules and synthetic schemes to improve the performance of the currently available $\bar{X}$ schemes in monitoring the process mean under the combined effect of measurement errors and autocorrelation are proposed. To maximize the detection ability of the 2-*of*-(*H*+1) runs-rules and synthetic schemes, we implement the modified side-sensitive (MSS) design approach for the charting regions as we show it yields the best possible performance out of all the available designs. These new monitoring schemes incorporate the additive model with a constant standard deviation and a first-order autoregressive model to the computation of the control limits in order to account for measurement errors and autocorrelation, respectively. Moreover, to construct a dedicated Markov chain matrix, the abovementioned models and some sampling methods are incorporated into the values of probability elements which are then used to derive closed-form expressions for the zero- and steady-state run-length distribution. This study is important because the majority of research tends to assume that observations are independent and identically distributed (i.i.d.) and that none of the measurements taken on the inspected items are contaminated, which is not always the case in real-life application. That is, a combined effect autocorrelation and measurement errors is a significant factor in quality and reliability statistics – hence an improved monitoring scheme for this scenario is discussed here. A real-life example is used to illustrate the practical implementation of the proposed schemes.

**Keywords:** Runs-rules, Measurement errors, First-order autoregressive model, Skip sampling strategy, Additive model, Multiple measurements sampling strategy, Zero-state, Steady-state, Markov chain.

## 1. Introduction

The main objective of statistical process monitoring (SPM) is to improve a monitoring process by detecting, identifying and removing any significant causes of variation. This is done by using a monitoring scheme (commonly known as control chart) to distinguish between chance causes of variation and assignable causes of variation. When only common causes of variation are present, the process is said to be in-control (IC). Otherwise, the process is said to be out-of-control (OOC) and assignable causes of variation have to be searched for. The most popular and simple monitoring schemes are the Shewhart charts, proposed by Walter A. Shewhart in the 1920's. Despite their simplicity and adaptability, the main shortcoming of Shewhart charts is their insensitivity in

*Corresponding author. E-mail: sandile@tuks.co.za;

[1]Department of Statistics, College of Science, Engineering and Technology, University of South Africa; Pretoria, South Africa; [2]Université de Nantes & LS2N UMR CNRS 6004, Département Qualité Logistique Industrielle et Organisation Nantes, France.

detecting small to moderate size shifts. Moreover, real life properties like, autocorrelation and measurement errors, tend to add more negative effect to the latter mentioned insensitivity in detecting small to moderate shifts.

One of the methods used to enhance the performance of the basic Shewhart scheme is to combine its operation with the conforming run-length (CRL) scheme – this yields a class of monitoring schemes called synthetic schemes, first proposed by Wu and Spedding (2000) and more recently reviewed by Rakitzis et al. (2019). The *CRL* is defined as the number of samples observed between two consecutive nonconforming samples, inclusive of the nonconforming sample at the end, which was proposed by Bourke (1991). This scheme gives an OOC signal when the *CRL* value is significantly small, say, $CRL \leq H$, where $H$ is a positive integer greater than 0. The main difference between a basic Shewhart scheme and a synthetic scheme is that the latter does not issue OOC signal at the first sample point that falls on the nonconforming regions. That is, the process waits until a second sample point falls on the nonconforming region and if these two nonconforming samples are relatively close to each other, then the CRL scheme signals and thus, an OOC signal is triggered. The rationale behind the CRL scheme is the following: small *CRL* values are indicative of less conforming items produced between the two successive nonconforming ones. Consequently, this may be an indication that the process is operating under some assignable causes of variation. Approximately 100 publications on synthetic schemes were reviewed in Rakitzis et al. (2019); here are some of the publications that were not covered, and some that are more recent: Khilare and Shirke (2010, 2012, 2015), Pawar and Shirke (2010), Ghute and Shirke (2012), Malela-Majika and Rapoo (2017), Pawar, Shirke and Khilare (2018), Shongwe and Graham (2019a), Haq (2019), Khaw et al. (2019), Shongwe et al. (2019a), Tran et al. (2019), Malela-Majika (2019), Raza, Nawaz and Han (2019), Haq and Khoo (2019).

In the SPM literature, a majority of research works does not account for measurement system errors, that is, it is usually assumed that none of the measurements taken on the inspected items are contaminated, see for example, Yeong et al. (2017), Sabahno et al. (2019), Tang et al (2019), Tran et al. (2019), etc. Maleki et al. (2017) argues that wherever there is a human involvement, an exact measurement is a rare phenomenon in any manufacturing and service environment; hence a difference between the real quantities and the measured ones will always exist even with highly sophisticated advanced measuring instruments. For a more thorough discussion on measurement errors, models used to capture the measurement system inaccuracy and the corresponding remedial approaches to reduce the negative effect thereof; readers must consult the articles cited in the review

by Maleki et al. (2017). In this paper, we use the additive model with a constant standard deviation which was first proposed by Linna and Woodall (2001) and the *m*-measurements remedial approach.

Autocorrelation within a subgroup sample is usually captured by some appropriate time series model. Box et al. (2008) outlines a number of these different non- and stationary time series models, e.g. autoregressive (AR), moving average (MA), autoregressive moving average (ARMA), autoregressive integrated moving average (ARIMA), etc. In this paper, we only consider the well-known first-order AR model (i.e. AR(1)) as a starting point (other models will be discussed in upcoming articles). The AR(1) model is the most commonly used time series model in SPM applications due to its simplicity as compared to other stationary time series models. The stationarity property of the AR(1) model is used to check whether the process is IC or not. That is, if the process remains in equilibrium around the constant mean then it is IC; however, when there is any statistically significant difference from the constant mean, it implies that the autocorrelated process is OOC. For some other discussions on AR(1) model in a univariate or multivariate SPM context, see for example: Claro, Costa and Machado (2008), Kazemzadeh et al. (2010), Costa and Machado (2011), Costa and Castagliola (2011), Chang and Wu (2011), Keramatpour et al. (2014), Franco et al. (2014a,b), Leoni et al (2015a,b,c), Hu and Sun (2015), Osei-Aning et al. (2017), Garza-Venegas et al. (2018), Shongwe et al. (2019a,b), Dargopatil and Ghute (2019), Ahmad et al. (2019), etc.

The synthetic-type schemes were shown to have four categories in Rakitzis et al. (2019). Shongwe and Graham (2018) showed that the 2-*of*-(*H*+1) runs-rules schemes also have four categories. These are termed non-side-sensitive (NSS), standard side-sensitive (SSS), revised side-sensitive (RSS) and modified side-sensitive (MSS) design approaches. These synthetic-type schemes denoted as S1, S2, S3 and S4 were first proposed by Wu and Spedding (2000), Davis and Woodall (2002), Machado and Costa (2014) and, Shongwe and Graham (2018), respectively. The runs-rules NSS, SSS, RSS and MSS were first proposed in Derman and Ross (1997), Klein (2000), adopted from Machado and Costa (2014) and, Antzoulakos and Rakitzis (2008) – which are denoted by RR1, RR2, RR3 and RR4, respectively. To the authors' best knowledge, only about five publications currently exist that investigate the combined effect of autocorrelation and measurement errors in different univariate SPM contexts; and these are: Scagliarini (2002, 2010), Yang and Yang (2005), Xiaohong and Zhaojun (2009) and, Costa and Castagliola (2011). Therefore, the main objective of this paper is to improve the Shewhart $\bar{X}$ scheme with a combined effect of measurement errors and autocorrelation (discussed in Costa and Castagliola, 2011) by: (i) Integrating its operation with the CRL scheme to form a synthetic $\bar{X}$ scheme, and (ii) Adding supplementary rules to form a 2-*of*-(*H*+1) $\bar{X}$ runs-rules schemes. More importantly, in order to gain maximum performance from the synthetic and runs-

rules schemes, we use the MSS design – as it yields the best possible performance out of the all four existing designs. Moreover, following on Davis and Woodall (2002) deduction that synthetic schemes are the same as the 2-*of*-(*H*+1) runs-rules schemes with a head-start feature, this property is used to construct a dedicated Markov chain matrix that is used to derive some zero- and steady-state closed-form expressions for both the MSS runs-rules and synthetic $\bar{X}$ schemes. Finally, the additive model with a constant standard deviation and the AR(1) model with constant standard deviation are used to account for the measurement errors and autocorrelation, respectively. To reduce the combined negative effect of measurement errors and autocorrelation, a sampling strategy that allows for multiple measurements per item and skipping some successive observations is incorporated in the probability values of the dedicated Markov chain matrix.

The rest of the paper is structured as follows: In Section 2, the properties of Shewhart $\bar{X}$ schemes with the effect of measurement errors and autocorrelation are discussed. The operation, construction of the Markov chain matrix and run-length properties of the proposed MSS runs-rules and synthetic schemes are discussed in Section 3. Empirical discussion of the proposed scheme and comparisons with the existing Shewhart $\bar{X}$ scheme is done in Section 4, and more specifically, in Section 4.4, the four design approaches are empirically compared to show the superiority of the MSS design. The practical implementation of the proposed schemes is given in Section 5 and finally, the concluding remarks are given in Section 6.

## 2. Measurement errors and autocorrelation for the Shewhart $\bar{X}$ scheme

### 2.1 Measurement errors

Assume that the $Y_{t,i}$ is a sequence of i.i.d. observations from a $N(\mu_0, \sigma_0)$ distribution (where $\mu_0$ and $\sigma_0$ are the nominal IC process mean and standard deviation, respectively) that are not directly observable, but can only be assessed from the results $\{X_{t,i,j}: t \geq 1;\ i = 1,2,\ldots,n;\ \ j = 1,2,\ldots,m\}$, with each element of the latter sequence expressed in terms of the additive model with a constant standard deviation, see Linna and Woodall (2001), i.e.,

$$X_{t,i,j} = A + BY_{t,i} + e_{t,i,j}; \qquad (1)$$

where $e_{t,i,j} \sim N(0, \sigma_M)$ is a random error term due to measurement inaccuracy and $\sigma_M$ is the standard deviation of the measurement system; for a sake of simplicity, in this paper, we will assume that $A$=0 and $B$=1, where $A$ and $B$ are two constants depending on the measurement system location error. Hence, the plotting statistic is the corresponding sample mean, which is given by

$$\bar{X}_t = \frac{1}{mn}\sum_{i=1}^{n}\sum_{j=1}^{m} X_{t,i,j} = \frac{1}{n}\left(\sum_{i=1}^{n} Y_{t,i} + \frac{1}{m}\sum_{i=1}^{n}\sum_{j=1}^{m} e_{t,i,j}\right). \quad (2)$$

That is, at each sampling point, there are *m* separate measurements, each of size *n* (i.e. a total of $m \times n$ observations). The standard deviation of the process in Equation (2) at each sampling point is given by

$$\sigma(\bar{X}_t) = \sqrt{\frac{\sigma_0^2}{n} + \frac{\sigma_M^2}{nm}} = \frac{\sigma_0}{\sqrt{n}C_1(m,\gamma)} \quad (3)$$

where $C_1(m,\gamma) = \sqrt{\frac{m}{m+\gamma^2}}$ and $\gamma = \frac{\sigma_M}{\sigma_0}$ denotes the ratio of the measurement system variability and the process variability, see Costa and Castagliola (2011). When $\bar{X}_t$ is from an imperfect measurement system, i.e. $\gamma > 0$, then we assume that multiple measurements (i.e. *m*-measurement strategy, with *m* > 1) are available for each i.i.d. subgroup sample.

### 2.2 Autocorrelated data using AR(1) model

Assume that the quality characteristic $\{Y_{t,i}: t \geq 1;\ i = 1, 2,\ldots, n\}$ is a sequence of samples from an autocorrelated $N(\mu_0, \sigma_0)$ distribution that fits a stationary AR(1) model, given by

$$Y_{t,i} - \mu_0 = \phi\left(Y_{t,i-1} - \mu_0\right) + \varepsilon_i;\ \ i = 1, 2, 3, 4,\ldots, n; \quad (4)$$

i.e. the current observation, $Y_{t,i}$, of the time series depends on the previous observation, $Y_{t,i-1}$; with a specified parameter $\phi$ (called a level of autocorrelation), where $|\phi| < 1$, $\varepsilon_i$ are i.i.d. normal (0, $\sigma_\varepsilon$) random variables; where $\mu_0$ and $\sigma_0$ are the nominal IC mean and standard deviation process parameters, respectively, where $\sigma_0 = \frac{\sigma_\varepsilon}{\sqrt{1-\phi^2}}$, and without loss of generality, assume $\sigma_\varepsilon = 1$; see Alwan and Radson (1992). After the occurrence of assignable causes, the process mean shifts from $\mu_0$ to $\mu_1 = \mu_0 + \delta\sigma_0$, so that $\delta = \frac{\mu_1 - \mu_0}{\sigma_0}$. Sampling techniques that involve skipping some of the successive observations (i.e. sampling of non-neighboring observations) have been shown to reduce serial dependence in time series data, see for example: Gilbert et al. (1993), Costa and Castagliola (2011), Franco et al. (2014b), Hu and Sun (2015), Leoni et al. (2015a), Dargopatil and Ghute (2019), Shongwe et al. (2019a,b). Consequently, the corresponding process with *s*-skipping sampling strategy remains an AR(1) process; however, defined as $\{Y_{t,i}: t \geq 1;\ i = 1, s{+}2, 2s{+}3, 3s{+}4,\ldots\}$ with parameter $\phi^{s+1}$:

$$Y_{t,i} - \mu_0 = \phi^{s+1}\left(Y_{t,i-s-1} - \mu_0\right) + \varepsilon_i';\ \ i = 1, s{+}2, 2s{+}3, 3s{+}4, \ldots \quad (5)$$

with $\varepsilon_i' = \varepsilon_i + \phi\varepsilon_{i-1} + \phi^2\varepsilon_{i-2} + \cdots + \phi^s\varepsilon_{i-s}$. Assuming that $\bar{Y}_t = \frac{1}{n}\sum_{i=1}^{n} Y_{t,(s+1)i-s}$ is the plotting statistic at sampling point *t*, then the standard deviation of the process in Equation (5) is given by

$$\sigma(\bar{Y}_t) = \frac{\sigma_0}{\sqrt{n}C_2(n,s,\phi)}; \tag{6}$$

with $C_2(n,s,\phi) = \sqrt{\frac{n}{n+2\left(\frac{\phi^{(s+1)(n+1)} - n\phi^{2s+2} + (n-1)\phi^{s+1}}{(\phi^{s+1}-1)^2}\right)}}$.

### 2.3 Combined effect of autocorrelation and measurement errors

Next, assume that the autocorrelated $Y_{t,i}$ (from Equation (5)) are not directly observable, that is, it can only be assessed from the results $\{X_{t,i,j}: t \geq 1;\ i = 1,2,\ldots,n;\ \ j = 1,2,\ldots,m\}$ from Equation (1). Note though, the $Y_{t,i}$ observations used in Equation (2) are no longer i.i.d., but are now autocorrelated. Moreover, we assume that $\bar{X}_t$ is from an imperfect measurement system, i.e. $\gamma > 0$, which means that there are several measurements available for each of the autocorrelated subgroup samples. Thus, the standard deviation of the plotting statistic in Equation (2) for an autocorrelated (with *s*-skip sampling strategy) and imperfect measurement system (with *m*-measurement sampling strategy), denoted hereafter as *s*&*m* strategy (with *s*>0 and *m*>1) at each sampling point, is given by

$$\sigma(\bar{X}_t) = \frac{\sigma_0}{\sqrt{n}C_3(m,n,\gamma,s,\phi)}; \tag{7}$$

with $C_3(m,n,\gamma,s,\phi) = 1\Big/\sqrt{\frac{1}{C_1^2(m,\gamma)} + \frac{1}{C_2^2(n,s,\phi)} - 1}$, where $C_1(m,\gamma)$ and $C_2(n,s,\phi)$ are as given in Equations (3) and (6), respectively.

## 3. Operation and run-length properties of the MSS runs-rules and synthetic schemes

### 3.1 Operation

Subgroup samples are usually taken at each sampling point to be inspected and then each of these samples are classified as either conforming or nonconforming depending on where the charting statistic plots on the charting regions shown in Figure 1. Note that a sample plots on a conforming region when it is under the influence of common causes of variation only; however, when it plots on a nonconforming region, it implies that it has some assignable causes of variation present. For any *s*&*m* strategy sampling scheme, the charting limits shown in Figure 1, i.e. the upper / lower control limit denoted by ($UCL/LCL$) and the center line ($CL$), are given by:

$$UCL/LCL = \mu_0 \pm k\sigma(\bar{X}_t) \text{ and } CL = \mu_0, \tag{8}$$

where $k > 0$ is the design parameter that is related to the distance from the center line to the $UCL/LCL$ in terms of the standard deviation, respectively.

<Insert Figure 1>

The operational procedure of the MSS runs-rules and synthetic *s&m* schemes are given in Table 1; where $CRL^{+}$ ($CRL^{-}$) is the number of conforming samples that fall in Region $B^{+}$ (Region $B^{-}$), which are in between the two nonconforming samples that fall in Region $A^{+}$ (Region $A^{-}$), including the nonconforming sample at the end, respectively. Moreover, the metric average run-length (*ARL*) is the average number of subgroup samples that are required before the first OOC signal is issued by a monitoring scheme, and $ARL_0$ denotes the desired nominal *ARL*.

<Insert Table 1>

### 3.2 Transition probability matrix

For the MSS runs-rules and synthetic schemes, there are two nonconforming regions (i.e. region $A^{+}$: upper, and region $A^{-}$: lower) and two conforming regions (i.e. region $B^{+}$: upper and region $B^{-}$: lower). Assume that $p_\theta = P(\bar{X}_i \in \theta)$ denotes the probability that a sample point plots in region $\theta \in \{A^{-}, A^{+}, B^{-}, B^{+}\}$, then given the charting regions in Figure 1, the probability of a charting statistic falling in each region is given by

$$\begin{aligned} p_{A^+} &= 1 - \Phi\left(k - \delta\sqrt{n}C_3(m,n,\gamma,s,\phi)\right) \\ p_{B^+} &= \Phi\left(k - \delta\sqrt{n}C_3(m,n,\gamma,s,\phi)\right) - \Phi\left(-\delta\sqrt{n}C_3(m,n,\gamma,s,\phi)\right) \\ p_{B^-} &= \Phi\left(-\delta\sqrt{n}C_3(m,n,\gamma,s,\phi)\right) - \Phi\left(-k - \delta\sqrt{n}C_3(m,n,\gamma,s,\phi)\right) \\ p_{A^-} &= \Phi\left(-k - \delta\sqrt{n}C_3(m,n,\gamma,s,\phi)\right), \end{aligned} \tag{9}$$

where $\Phi(\cdot)$ denotes the cumulative distribution function (c.d.f.) of the standard normal distribution. Let '±' denote a state that a charting statistic at time zero falls in a nonconforming region, that is, the charting statistic falls either in region $A^{-}$ or region $A^{+}$ at the beginning of the monitoring process; this assumption is referred to as the "head-start feature" of the synthetic scheme – see Davis and Woodall (2002), Knoth (2016), Shongwe and Graham (2018) and Rakitzis et al (2019) for a more thorough discussion on this. For instance, '$\pm A^{-}$' implies that at time 0, we assume the charting statistic plots either in region $A^{-}$ or region $A^{+}$, and then at sampling time $t$ = 1, the charting statistic plots in region $A^{-}$.

Next, the steps involved in constructing the TPMs of the MSS runs-rules and synthetic *s&m* scheme are as follows for any integer value of $H > 0$:

- Step (i) Determine all the absorbing states that lead to an OOC signal; those with and without head-start are denoted by $\Psi$ and $\Lambda$, respectively.
- Step (ii) Decompose the states in Step (i) into transient states by removing the last nonconforming element, where those with and without head-start are denoted by $\psi$ and $\eta$, respectively.

- Step (iii) The transient state corresponding to the IC regions is defined as $\varphi = \eta_{H+1}$.
- Step (iv) Define the state space, denoted by $\Omega$, which is a union of the states defined in Steps (i) to (iii).

Hence, for illustrative purpose, assume $H = 2$, then the state space using the steps outlined above is constructed as follows:

- Step (i) yields $\Lambda_1=\{A^+A^+\}$, $\Lambda_2=\{A^+B^+A^+\}$, $\Lambda_3=\{A^-A^-\}$, $\Lambda_4=\{A^-B^-A^-\}$ and $\Psi_1=\{\pm A^+\}$, $\Psi_2=\{\pm A^-\}$, $\Psi_3=\{\pm B^+A^+\}$, $\Psi_4=\{\pm B^-A^-\}$.
- Step (ii) yields $\eta_1=\{A^+B^+\}$, $\eta_2=\{A^+\}$, $\eta_4=\{A^-\}$, $\eta_5=\{A^-B^-\}$ and $\psi_1=\{\pm\}$, $\psi_2=\{\pm B^+\}$, $\psi_3=\{\pm B^-\}$.
- Step (iii) yields $\varphi = \eta_3 =\{B^-, B^+\}$.
- Step (iv) yields $\Omega \equiv\{\eta_1,\eta_2;\varphi;\eta_4,\eta_5;\psi_1,\psi_2,\psi_3;\text{OOC}\}$.

Consequently, the resulting Markov chain TPM is given by

| | $\eta_1$ | $\eta_2$ | $\varphi$ | $\eta_4$ | $\eta_5$ | $\psi_1$ | $\psi_2$ | $\psi_3$ | OOC |
|---|---|---|---|---|---|---|---|---|---|
| $\eta_1$ | | | $p_{B^+}+p_{B^-}$ | $p_{A^-}$ | | | | | $p_{A^+}$ |
| $\eta_2$ | $p_{B^+}$ | | $p_{B^-}$ | $p_{A^-}$ | | | | | $p_{A^+}$ |
| $\varphi$ | | $p_{A^+}$ | $p_{B^+}+p_{B^-}$ | $p_{A^-}$ | | | | | |
| $\eta_4$ | | $p_{A^+}$ | $p_{B^+}$ | | $p_{B^-}$ | | | | $p_{A^-}$ |
| $\eta_5$ | | $p_{A^+}$ | $p_{B^+}+p_{B^-}$ | | | | | | $p_{A^-}$ |
| $\psi_1$ | | | | | | | $p_{B^+}$ | $p_{B^-}$ | $p_{A^+}+p_{A^-}$ |
| $\psi_2$ | | | $p_{B^+}+p_{B^-}$ | $p_{A^-}$ | | | | | $p_{A^+}$ |
| $\psi_3$ | | $p_{A^+}$ | $p_{B^+}+p_{B^-}$ | | | | | | $p_{A^-}$ |
| OOC | | | | | | | | | 1 |

Based on the latter TPM, it is apparent that its structure is such that for any positive integer $H$>0, it is given by a $(M+1)\times(M+1)$ matrix $\mathbf{P}$, defined as

$$\mathbf{P} = \begin{pmatrix} \mathbf{Q} & \mathbf{r} \\ \mathbf{0}' & 1 \end{pmatrix} \tag{10}$$

where $\mathbf{Q}$ is the $M \times M$ matrix of transient states (i.e. essential TPM), the $M \times 1$ vector $\mathbf{r}$ is such that $\mathbf{r} = \mathbf{1} - \mathbf{Q1}$, i.e. each row sums to 1, with $M \times 1$ vectors $\mathbf{1} = (1\ 1\ \ldots\ 1)'$ and $\mathbf{0} = (0\ 0\ \ldots\ 0)'$. Moreover, the breakdown of the TPM for $H = 2$ (and other integer values of $H$ – not shown here), indicate that the dimension of the TPMs for any $H > 0$ is given by $M = \tau + \kappa$ for the MSS synthetic scheme, where $\tau = 2H + 1$ and $\kappa = 2H - 1$. To obtain TPMs with an obvious recursive pattern for any $H > 0$, we define the state space, $\Omega$, as follows,

$$\Omega = \{\eta_1,\ldots,\eta_{\frac{(\tau+1)}{2}-1}, \eta_{\frac{(\tau+1)}{2}} \equiv \varphi, \eta_{\frac{(\tau+1)}{2}+1}, \ldots, \eta_\tau; \psi_1, \ldots, \psi_\kappa; \text{OOC}\}. \tag{11}$$

On the contrary, the dimension of the TPMs of the MSS runs-rules schemes, for any $H > 0$ is given by $M = \tau$, where $\tau = 2H + 1$ and $\kappa = 0$; as the head-start feature elements are not applicable in the design of the MSS runs-rules. Consequently, the Ω for the MSS runs-rules scheme is given by,

$$\Omega = \{\eta_1,\ldots, \eta_{\frac{(\tau+1)}{2}-1}, \eta_{\frac{(\tau+1)}{2}} \equiv \varphi, \eta_{\frac{(\tau+1)}{2}+1}, \ldots, \eta_\tau; \text{OOC}\}. \quad (12)$$

Therefore, it follows that the TPM of MSS synthetic scheme is given in Table 2. Moreover, by removing the head-start elements, i.e. $\psi_1$, …, $\psi_\kappa$ in Table 2, then the resulting TPM corresponds to that of the MSS runs-rules scheme.

<Insert Table 2>

### 3.3 Some general run-length properties

Since the TPMs of the MSS runs-rules and synthetic schemes for any possible integer value of $H$ have been determined, then important properties of the run-length ($RL$) can be determined via an appropriate Markov chain technique, see Chapter 4 in Fu and Lou (2003). That is, the $ARL$ = E($RL$) and the standard deviation of the $RL$ ($SDRL = \sigma(RL)$) are defined as

$$ARL = \boldsymbol{\xi}^{\mathrm{T}}\mathbf{R} \quad (13)$$

$$SDRL = \sqrt{2\boldsymbol{\xi}^{\mathrm{T}}(\mathbf{I}-\mathbf{Q})^{-2}\mathbf{Q}\mathbf{1} - ARL^2 + ARL}, \quad (14)$$

where $\boldsymbol{\xi}$ denotes either the $M \times 1$ zero- or steady-state initial probability vector; and $\mathbf{R}$ is a $M \times 1$ vector containing $ARL$ values of being in each of the $M$ transient states, and it is given by

$$\mathbf{R} = (\mathbf{I}-\mathbf{Q})^{-1}\mathbf{1}. \quad (15)$$

Using the $\mathbf{Q}$ from Table 2, Equation (15) becomes,

$$\mathbf{R} \equiv \mathbf{R}^{\text{no HS}}//\mathbf{R}^{\text{HS}}. \quad (16)$$

where, $\mathbf{R}^{\text{no HS}}$ is a $\tau \times 1$ vector containing $ARL$ values of being in each of the states without the head-start feature, $\mathbf{R}^{\text{HS}}$ is a $\kappa \times 1$ vector containing $ARL$ values of being in each of the states with the head-start feature and '//' denotes the vertical concatenation operator. The components of the $ARL$ vector in Equation (16) are given by

$$\mathbf{R}^{\text{no HS}} = \begin{pmatrix} \varsigma_1 \\ \varsigma_2 \\ \vdots \\ \varsigma_{H-3} \\ \varsigma_{H-2} \\ \varsigma_{H-1} \\ \varsigma_H \\ \varphi = \varsigma_{H+1} \\ \varsigma_{H+2} \\ \varsigma_{H+3} \\ \varsigma_{H+4} \\ \varsigma_{H+5} \\ \vdots \\ \varsigma_{2H} \\ \varsigma_{2H+1} \end{pmatrix} = \frac{1}{\mathrm{G}} \begin{pmatrix} (1+p_A W_B^1)(1+p_D W_C^0) \\ (1+p_A W_B^2)(1+p_D W_C^0) \\ \vdots \\ (1+p_A W_B^{H-3})(1+p_D W_C^0) \\ (1+p_A W_B^{H-2})(1+p_D W_C^0) \\ (1+p_A W_B^{H-1})(1+p_D W_C^0) \\ 1+p_D W_C^0 \\ (1+p_A W_B^0)(1+p_D W_C^0) \\ 1+p_A W_B^0 \\ (1+p_D W_C^{H-1})(1+p_A W_B^0) \\ (1+p_D W_C^{H-2})(1+p_A W_B^0) \\ (1+p_D W_C^{H-3})(1+p_A W_B^0) \\ \vdots \\ (1+p_D W_C^2)(1+p_A W_B^0) \\ (1+p_D W_C^1)(1+p_A W_B^0) \end{pmatrix} \tag{17}$$

and

$$\mathbf{R}^{\text{HS}} = \begin{pmatrix} \psi_1 = \varsigma_{2H+2} \\ \varsigma_{2H+3} \\ \varsigma_{2H+4} \\ \varsigma_{2H+5} \\ \varsigma_{2H+6} \\ \varsigma_{2H+7} \\ \varsigma_{2H+8} \\ \vdots \\ \varsigma_{4H-3} \\ \varsigma_{4H-2} \\ \varsigma_{4H-1} \\ \varsigma_{4H} \end{pmatrix} = \frac{1}{G} \begin{pmatrix} 1-p_A p_D W_B^0 W_C^0 \\ (1+p_A W_B^{H-1})(1+p_D W_C^0) \\ (1+p_D W_C^{H-1})(1+p_A W_B^0) \\ (1+p_A W_B^{H-2})(1+p_D W_C^0) \\ (1+p_D W_C^{H-2})(1+p_A W_B^0) \\ (1+p_A W_B^{H-3})(1+p_D W_C^0) \\ (1+p_D W_C^{H-3})(1+p_A W_B^0) \\ \vdots \\ (1+p_A W_B^2)(1+p_D W_C^0) \\ (1+p_D W_B^2)(1+p_A W_B^0) \\ (1+p_A W_B^1)(1+p_D W_C^0) \\ (1+p_D W_C^1)(1+p_A W_B^0) \end{pmatrix} \tag{18}$$

where $G$ is given by

$$\mathrm{G} = 1 - p_A(p_C + p_D + p_D p_C W_C^0) - p_B(1 + p_D W_C^0) - p_C - p_A p_B^H(1 + p_D W_C^0) - p_D p_C^H - p_A W_B^1(p_C + p_D + p_C p_D W_C^0),$$

with $W_B^r = p_B^r\left(\frac{1-p_B^{H-r}}{1-p_B}\right)$, $W_C^r = p_C^r\left(\frac{1-p_C^{H-r}}{1-p_C}\right)$, $r = 0,1,2,\ldots,H-1$.

### 3.4 Zero-state run-length properties for the MSS runs-rules and synthetic schemes

In order to compute the zero-state run-length properties, the initial probability vector $\boldsymbol{\xi}^{\mathrm{T}} = \mathbf{q}^{\mathrm{T}} = (0,\ldots,0,1,0,\ldots,0)$ where the unique "1" is located

- the $\left(\frac{\tau+1}{2}\right)^{\text{th}}$ position of the $\mathbf{q}^{\mathrm{T}}$ vector, i.e. corresponding to '$\eta_{\frac{(\tau+1)}{2}} \equiv \varphi$' on the TPM in Table 2.
- the $(\tau+1)^{\text{th}}$ position of the $\mathbf{q}^{\mathrm{T}}$ vector, i.e. corresponding to '$\psi_1$' on the TPM in Table 2.

The zero-state *ARL* (*ZSARL*) is given by $ZSARL = \mathbf{q}^{\mathrm{T}}\mathbf{R}$, with $\mathbf{R}$ given in Equation (16) which yields the following closed-form expressions:

- for the MSS runs-rules *s&m* schemes

$$ZSARL = \frac{(1 + p_A W_B^0)(1 + p_D W_C^0)}{\mathrm{G}} = \frac{\left(1 + p_A\left(\frac{1 - p_B^H}{1 - p_B}\right)\right)\left(1 + p_D\left(\frac{1 - p_C^H}{1 - p_C}\right)\right)}{\mathrm{G}}. \tag{19}$$

- for the MSS synthetic s&m schemes

$$ZSARL = \frac{1 - p_A p_D W_B^0 W_C^0}{\mathrm{G}} = \frac{1 - p_A p_D\left(\frac{1 - p_B^H}{1 - p_B}\right)\left(\frac{1 - p_C^H}{1 - p_C}\right)}{\mathrm{G}}. \tag{20}$$

### 3.5 Steady-state run-length properties for the MSS runs-rules and synthetic schemes

In steady-state mode, the effect of a head-start disappears since the process has been running IC for a long time and thus, the corresponding components are discarded in the Markov chain matrix in Table 2, and consequently, the *ARL* vector in Equation (16) reduces to $\mathbf{R} \equiv \mathbf{R}^{\text{no HS}}$.

The steady-state non-zero initial probability vector (i.e. $\boldsymbol{\xi}^{\mathrm{T}} = \mathbf{u}^{\mathrm{T}}$) is computed while the process is IC; that is, $p_A = p_D$ and $p_B = p_C$ as $\delta = 0$. Let $q = p_A = p_D$ and $p = p_B = p_C$ when $\delta = 0$, then using Champ (1992) simplified cyclical steady-state method; the initial probability vector of the MSS runs-rules or synthetic *s&m* scheme is given by $\mathbf{u} = (\mathbf{1}'\mathbf{z})^{-1} \cdot \mathbf{z}$, where $\mathbf{z}$ is the $(2H - 1) \times 1$ vector given by $\mathbf{z} = (\mathbf{G} - \mathbf{Q}')^{-1}\mathbf{e}_{H+1}$, with the $(2H - 1) \times (2H - 1)$ matrix $\mathbf{G}$, given by $\mathbf{G} = \mathbf{q} \cdot \mathbf{1}' + \mathbf{I}$, where $\mathbf{e}_{H+1} = (0\ 0\ 0 \ldots 0\ 1\ 0\ \ldots 0\ 0\ 0)$, i.e., a $(H{+}1)^{\text{th}}$ unit vector. Thus, using the Markov chain matrix in Table 2 (without the head-start elements), then basic algebraic matrix manipulations yield:

$$\mathbf{u} = \begin{pmatrix} \mathrm{u}_1 \\ \mathrm{u}_2 \\ \mathrm{u}_3 \\ \vdots \\ \mathrm{u}_{\mathrm{H}-2} \\ \mathrm{u}_{\mathrm{H}-1} \\ \mathrm{u}_{\mathrm{H}} \\ \mathrm{u}_{\mathrm{H}+1} \\ \mathrm{u}_{\mathrm{H}+2} \\ \mathrm{u}_{\mathrm{H}+3} \\ \mathrm{u}_{\mathrm{H}+4} \\ \vdots \\ \mathrm{u}_{2\mathrm{H}-1} \\ \mathrm{u}_{2\mathrm{H}} \\ \mathrm{u}_{2\mathrm{H}+1} \end{pmatrix} = \frac{1 - p}{1 - p + q(1 - p^H)} \begin{pmatrix} qp^{H-1} \\ qp^{H-2} \\ qp^{H-3} \\ \vdots \\ qp^2 \\ qp \\ q \\ 1 - q\left(\frac{1 - p^H}{1 - p}\right) \\ q \\ qp \\ qp^2 \\ \vdots \\ qp^{H-3} \\ qp^{H-2} \\ qp^{H-1} \end{pmatrix}. \tag{21}$$

Thus, it follows that the steady-state *ARL* (*SSARL*) of the MSS runs-rules or synthetic *s&m* scheme is given by

$$SSARL = \mathrm{u}_{\mathrm{H}+1}\varsigma_{\mathrm{H}+1} + \sum_{r=1}^{H} \mathrm{u}_r \times \left(\varsigma_r + \varsigma_{(2H+2)-r}\right), \tag{22}$$

with $\varsigma_r$ defined in Equation (17) and $\mathrm{u}_r$ defined in Equation (21), for $r = 1, 2, \ldots, H$.

### 3.6 Overall performance metrics

In addition to specific shifts measures, i.e. Equations (19), (20) and (22), a number of researchers in the SPM literature (see for example, Reynolds and Lou (2010), Ryu, Wan and Kim (2010), Machado and Costa (2014), Tran, Castagliola and Balakrishnan (2017), Malela-Majika and Rapoo (2017), You (2017, 2018), Shongwe and Graham (2019b), etc.) have encouraged the use of some overall performance metrics, like the expected *ARL* (*EARL*) because users tend not to know beforehand what exact shift value(s) is targeted. The *EARL* measures the performance of a monitoring scheme over a range of shift values, i.e. $\delta_{\min}$ to $\delta_{\max}$ – which are the lower and the upper bound of $\delta$, respectively. Note that the shifts within the interval $[\delta_{\min}, \delta_{\max}]$ usually occur according to a p.m.f. equal to $U(\delta)$ which is usually unknown. In the absence of any particular information, it is usually assumed that the shifts in the process mean happen with equal probability, then $U(\delta) = 1/(\delta_{\max} - \delta_{\min})$ i.e. a uniform U($\delta_{\min}, \delta_{\max}$) distribution. Thus, following a similar design procedure as done by the latter authors, the MSS runs-rules and synthetic *s&m* schemes will be designed based on the optimal parameters ($H^*$, $k^*$) that yield the best overall performance for a range of specified shifts and it is achieved by using

$$(H^*, k^*) = \underset{(H,k)}{\operatorname{argmin}} EWRL$$

subject to

$$ARL(\delta = 0) = ARL_0 \tag{23}$$

with

$$EWRL = \int_{\delta_{\min}}^{\delta_{\max}} ARL(\delta)U(\delta)d\delta$$

with $ARL_0$ being the pre-specified nominal *ARL* and $\delta \in [\delta_{\min}, \delta_{\max}]$. That is, to choose the parameters that yield the smallest *EARL*, where $ARL(\delta)$ is the *ARL* as a function of the shift $\delta$ in the parameter under surveillance.

Finally, the performance comparison index (*PCI*), by Wu et al. (2008), will also be used to measure the relative effectiveness of two different schemes, which is given by

$$PCI = EARL_c/EARL_b, \tag{24}$$

where $EARL_b$ (denominator) is the *EARL* of the 'benchmark' scheme (i.e. the $\bar{X}$ *s&m* scheme of Costa and Castagliola (2011)) and $EARL_c$ (numerator) is the *EARL* of some other 'competing' scheme. When the $PCI$ is equal to 1, greater than 1 or less than 1, it implies that the $\bar{X}$ *s&m* scheme of Costa and Castagliola (2011) has the same, better or worse performance than the competing scheme, respectively.

## 4. Empirical discussion

### 4.1 IC design parameters

It is important to note that the design parameters do not depend on the level of autocorrelation or measurement inaccuracy. That is, the design parameters are the same as those for i.i.d. observations discussed in Shongwe and Graham (2018), where $ARL_0$ = 200, 370.4, 500 and 1000. For the MSS runs-rules (i.e. RR4) and MSS synthetic (i.e. S4) schemes, as $H$ increases, the values of $k$ converge to some specific value no matter how large $H$ gets (see boldfaced values in Table 3). Although not shown here (see Shongwe and Graham (2018)), for the NSS, SSS and RSS schemes, as $H$ increases, the value of $k$ keeps increasing also, that is, as $H$ gets very large, the value of $k$ approaches 3 at a slow rate (i.e. $k$ converges to the $\bar{X}$ scheme design parameter value of 3). A similar pattern is observed for other standard values of $ARL_0$.

<Insert Table 3>

### 4.2 Separate and combined effect of measurement errors and autocorrelation

In Table 4, we discuss the OOC performance of the basic $\bar{X}$, RR4 and S4 schemes under the i.i.d. case (no measurement errors or autocorrelation), separate and combined effect of the measurement errors and autocorrelation, i.e., $(\phi, \gamma) \in \{(0,0), (0,0.5), (0.5,0), (0.5,0.5)\}$, respectively. In each separate panel of the four scenarios, the basic $\bar{X}$ scheme is compared with the RR4 and S4 schemes in zero- and steady-state modes.

In each panel or each pair $(\phi, \gamma)$ in Table 4, with respect to *ARL*, the (zero- and steady-state) RR4 and (steady-state only) S4 schemes have a better OOC performance than the basic $\bar{X}$ scheme when $\delta \leq 1$; however, for $\delta > 1$ the converse is true. In zero-state, the S4 scheme has a uniformly better OOC *ARL* performance than the basic $\bar{X}$ scheme for all considered shift values. The *ARL* values at each shift value tend to increase as each of the parameters in the pair $(\phi, \gamma)$ increases. For example, when the measurement error increases from 0% to 50%, i.e. the pair $(\phi, \gamma)$ is increased from (0,0) to (0,0.5), the *ZSARL* at $\delta$=0.25 for the S4 scheme also increases from 54.9 to 69.9 – indicating a deteriorating process. Similarly, when the autocorrelation level is increased from 0% to 50%, i.e. the pair $(\phi, \gamma)$ is increased from (0,0) to (0.5,0), the *ZSARL* at $\delta$=0.25 increases from 54.9 to 118.7.

Moreover, when both the measurement error and autocorrelation are increased from 0 to 50%, i.e. the pair $(\phi, \gamma)$ is increased from (0,0) to (0.5,0.5), the *ZSARL* at $\delta$=0.25 increases from 54.9 to 128.9. Next, it is observed that for the S4 scheme, in the i.i.d. case, 50% measurement error only, 50% level of autocorrelation only and, combined 50% of measurement error and autocorrelation, respectively yields the zero-state *EARL* of 148.9, 155.5, 179.4 and 185.0 – indicative of a deteriorating process as the monitoring process is subjected to separately as well as combined measurement errors and autocorrelation.

The main deductions from Table 4 are the following:

- With respect to *EARL*, the RR4 and S4 schemes under the separate or combined effect of measurement errors and autocorrelation have a better performance than the basic $\bar{X}$ scheme. The latter is further illustrated by the fact that all the *PCI* values of considered schemes are lower than that of the basic $\bar{X}$ scheme.
- Separately, autocorrelation has a higher negative effect as compared to the negative effect of the measurement errors. Combined, they yield a much higher negative effect.
- The zero- and steady-state OOC performances of the RR4 schemes have *ARL* and *EARL* that are respectively very close to each other, this is summarized in Remark 1. This is further illustrated by the approximately equal values of the *PCI*s.

<Insert Table 4>

**Remark 1:** Let the zero- and steady-state *EARL* be denoted by *ZSEARL* and *SSEARL*, respectively; then the percentage difference (%Diff) is given by $\%\text{Diff} = \frac{ZSEARL - SSEARL}{SSEARL} \times 100\%$. Since the zero- and steady-state OOC performances of the RR4 schemes have the *ARL*s and *EARL*s that are respectively very close to each other, it is observed that their %Diff are always less than 1%. To preserve writing space, only the steady-state performance of the RR4 schemes is presented henceforth.

### 4.3 The MSS runs-rules and synthetic *s&m* schemes

To evaluate the effect of implementing the *s&m* strategy to reduce the combined effect of autocorrelation and measurement errors, let the 0&1 strategy denote the no remedial approach to reduce the combined effect of autocorrelation and measurement errors. Hence, 3&4 implies that the *s*=3 observations are skipped before sampling to form a rational subgroup and that *m*=4 measurements are taken per item.

<Insert Tables 5 and 6>

In Tables 5 and 6, the effect of using 3&4 strategy instead of the 0&1 strategy is studied in the case of the S4 and (RR4 and S4) in zero- and steady-state modes, respectively. Due to Remark 1, the RR4 scheme in zero-state is not shown here. The OOC performance illustration is shown for $H \in \{1,2,\ldots,12\}$ as per discussion in Table 3 to observe what happens to the *ARL* and *EARL* as $k$ approaches the convergence property. Moreover, to investigate what value of $H$ has the optimal overall performance gain (*OPG*) such that increasing $H$ does not yield any further significant *OPG*. To do so, two metrics are defined as follows,

$$\%\text{Diff} = \frac{EARL_{0\&1} - EARL_{3\&4}}{EARL_{3\&4}} \times 100\%, \qquad \text{for a given value of H}$$

$$\text{OPG}(H) = \frac{EARL_{H-1} - EARL_{H}}{EARL_{H}} \times 100\%, \qquad \text{for a specific values of s\&m;}$$

where $EARL_{0\&1}$ and $EARL_{H}$ denote the *EARL* of the 0&1 strategy (with $H$ fixed) and at a specific value of $H$ (with *s&m* fixed), respectively – the others are defined in a similar manner. In Tables 5 and 6, it is observed that increasing *s&m* from the 0&1 strategy to 3&4 strategy yields a performance gain of at least 20% for all considered values of $H$ when $\phi$=0.5, $\gamma$=0.5 and $n$=5. For example, in zero-state, the S4 scheme (in Table 5) shows that when $H$=1, the percentage gain of using the 3&4 strategy instead of the 0&1 strategy is 24.9%. Next, the *OPG* of using $H$=2 instead of $H$=1 when 0&1 and 3&4 sampling strategies are implemented are 5.9% and 4.4%, respectively. In Tables 5 and 6, it is observed that when $H$>5, the *OPG*s of the 0&1 strategy are all less than 1% indicating that increasing $H$ greater than 5 do not yield any more significant percentage gains; consequently, when $\phi$=0.5, $\gamma$=0.5 and $n$=5, the most ideal value of $H$ is equal to 5 and 4 for the 0&1 and 3&4 strategy, respectively. More importantly, it is observed that as $H$ approaches the values of $H$ where $k$ start to converge (see Table 3 for the convergence property, i.e. around $H$ equal to 11 and 12) the *OPG* approaches a percentage value of 0 – indicating that there is no benefit in overall performance, at all, by continually increasing the value of $H$ for the RR4 and S4 *s&m* schemes beyond the converged values of $k$ in both zero- and steady-state modes.

<Insert Tables 7 and 8>

Furthermore, in Tables 7 and 8, the *OPG* is further analyzed for a variety of levels of autocorrelation and measurement errors. Note though, due to space restriction, only the steady-state analysis of the RR4 and S4 *s&m* schemes when $H$=5, $n$=5, $\delta_{min}$=0, $\delta_{max}$=3, $m \in \{1,2,3,4\}$, $s \in \{0,1,2,3\}$ and $ARL_0$=370.4; where $\phi$=0.5, $\gamma \in \{0,0.1,0.2,\ldots,0.9\}$ in Table 7 and $\gamma$=0.5, $\phi \in \{0,0.1,0.2,\ldots,0.9\}$ in Table 8.

Firstly, in Table 7, the following is observed:

- When $\gamma$=0, since there are no measurement errors, the values of the *EARL* do not change for any integer value of $m \geq 1$. Since $\phi$=0.5, as $s$ increases from 0 to 3, the *EARL* values decrease (vertically downwards) indicating some improvement in OOC performance.
- With $s$ and $m$ fixed, when $\gamma$>0, the *EARL* tends to increase indicating a deteriorating process. However, for each given integer value of $s$, increasing $m$ leads to some minor decrease in the *EARL* value. For instance, when $s$=1 and $\gamma$=0.5, the overall performance gains are 1.9%, 0.6%, 0.3% when $m$ is increased from (1 to 2), (2 to 3), (3 to 4), respectively. This means that there is a 1.9% overall performance gain in taking measurements twice as compared to once. Similarly, there are 0.6% and 0.3% overall performance gains in taking measurements three and four times instead of two and three times, respectively.

Next, in Table 8, the following is observed:

- When $\phi$=0, (i.e. no autocorrelation), the *EARL* does not change for any integer value of $s \geq 0$. Moreover, since $\gamma$=0.5, as $m$ increases from 1 to 4, the *EARL* values decrease (vertically downwards) indicating an improvement in performance; note though, this improvement is at a lower rate than in Table 7.
- With $s$ and $m$ fixed, when $\phi$>0, the *EARL* tends to increase indicating a deteriorating process. However, for each given integer value of $m$, increasing $s$ leads to some decrease in the *EARL* values; this improvement is at a slightly higher rate than in Table 7. For instance, when $m$=1 and $\phi$=0.5, the overall performance gains are 10.5%, 4.3%, 1.9% when $s$ is increased from (0 to 1), (1 to 2), (2 to 3), respectively. This means that there is a 10.5% overall performance gain in skipping one observation as compared to successive sampling when forming a rational subgroup. Similarly, there are 4.3% and 1.9% overall performance gains in skipping two and three observations instead of one and two, respectively.

As similarly deduced in Table 4, an outlook comparison of Tables 7 and 8 indicates: (i) The autocorrelation level (with $\gamma$ fixed) has a significantly greater negative effect on the RR4 and S4 *s&m* schemes performances than the measurement error level, and (ii) The *s*-skip strategy has a greater remedial effect than the *m*-multiple measurement strategy in improving the performance of the RR4 and S4 *s&m* schemes.

Therefore, based on the analysis done in this section, the recommended values of $H$, $s$ and $m$ are discussed next. For all different specific shifts values of $\delta$, a value of $H$ that is more or less around the neighborhood of 5 is recommended. Note though, for large shifts, $H$ much lower than 5 is recommended. For any $\phi$ value, when $\gamma$ is approximately around (0, 0.3), (0.3, 0.7) and (0.7, 1) an $m$ equal to 1, 2 and 3 are recommended, respectively. For any $\gamma$ value, when $\phi$ is approximately around

(0, 0.3), (0.3, 0.6) and (0.6, 1) an $s$ value equal to 1, 2 and 3, are recommended, respectively. Note that values of $s$ and $m$ greater than 3 are not recommended so as to not violate the concept of rational subgroup and repeatability & reproducibility (R&R) discussed in Costa and Castagliola (2011). Note though, in an unlikely event that a process has a large number of observations and an abundance of measurement instruments, then the use of $s$ or $m$ greater than 3 is recommended.

### 4.4 Comparison with other runs-type and synthetic-type *s&m* schemes

Note that in this paper, we focused on the RR4 and S4 *s&m* monitoring schemes because as it is shown in this section that these MSS designs yields a uniformly better performance than the NSS, SSS and RSS designs. For the sake of illustration, in Table 9 we assume that $H$=5, $\gamma$=0.7, $\phi$=0.7, $n \in \{3,10\}$, $s \in \{0,3\}$ and $m \in \{1,4\}$. Since in steady-state, RR1≡S1, RR2≡S2, RR3≡S3 and RR4≡S4 – see Shongwe and Graham (2019a), the corresponding $k$ values such that the actual IC *ARL* is equal to 370.4 are 2.2395, 2.1117, 2.1056 and 1.9168, respectively. Assuming a uniform distribution in $\delta$, then the average ratio of *ARL*s (*ARARL*) is defined by (see Wu et al., 2008):

$$ARARL = \frac{1}{\Delta}\sum_{\delta_{min}}^{\delta_{max}} \frac{ARL_c(\delta)}{ARL_{MSS}(\delta)},$$

where $\Delta$ is the number of increment steps from $\delta_{min}$ to $\delta_{max}$, $ARL_{MSS}(\delta)$ is the *ARL* produced by the MSS (i.e. RR4 or S4) scheme for a specific *s&m* strategy and $ARL_c(\delta)$ is the *ARL* of some specified competing scheme for the same *s&m* strategy. If the value of *ARARL* is larger than one, the competing scheme will produce larger OOC *ARL* over a larger shift range and / or to a larger degree compared to the MSS scheme and thus, the competing scheme is relatively less effective. However, if the *ARARL* is smaller than one, the competing scheme will have higher overall effectiveness than the MSS scheme. Finally, if the value of *ARARL* is equal to one, the competing scheme has a similar overall performance with the MSS scheme. In Table 9, the following is observed:

- Separately, for the 0&1 and 3&4 strategy, it is observed that in general, with respect to *ARL*, *EARL* and *ARARL*, the performance of these schemes can be sorted as follows - RR1≡S1 < RR2≡S2 < RR3≡S3 < RR4≡S4. For example, when $n$=10 and $\delta$=0.25, then each of the scheme's 3&4 strategy yields *ARL* values of 93.8, 65.2, 64.2 and 54.3, respectively. Moreover, the corresponding *EARL* values are 169.1, 157.8, 157.5 and 152.9, respectively. The *ARARL*s of the NSS, SSS and RSS schemes are 26%, 10% and 9% higher than those of the MSS schemes for the 0&1 strategy when $n$=3; however, for the 3&4 strategy these are 36%, 14% and 13% higher than those of the MSS schemes, respectively.

- For each scheme, the implementation of the *s&m* sampling strategy yields improved performance as long as $\phi$>0 and $\gamma$>0. For example, when $n$=10, the RR1 or S1 scheme yields a 36.5% improvement in the process when implementing the 3&4 strategy instead of the 0&1 strategy.
- Increasing the sample size improves the detection ability of all schemes by a similar proportion so that the order in the best detection ability is unchanged, i.e. RR1≡S1 < RR2≡S2 < RR3≡S3 < RR4≡S4.

<Insert Table 9>

Similar (but in a different context) to the deductions made for the i.i.d. case in Shongwe and Graham (2018); the RR4 and S4 *s&m* schemes yield the best OOC performance than the corresponding competitors when the process is under the effect of both autocorrelation and measurement errors. Although not shown here, a similar conclusion is observed for the individual effect of autocorrelation or measurement errors, as well as in the zero-state mode. Moreover, we observed that Remark 1 holds for the RR1, RR2 and RR3 schemes.

Therefore, this is the reason why the focus of this paper was mainly on the MSS (i.e. the RR4 and S4) schemes only – this is the best possible design for the 2-*of*-(*H*+1) runs-rules and synthetic *s&m* schemes in both the zero- and steady-state modes, for all possible integer values of *H*.

## 5. Illustrative example

The yoghurt cup filling process dataset taken from Costa and Castagliola (2011, p.670) is displayed on Table 10, which shows the weights of different yoghurt cups taken at different sampling points. The dataset has 20 samples (each of size 5 yoghurt cups taken every hour and each weighted *m*=2 times) corresponding to a 20-hours sequence of production. The Phase I analysis of this process indicated that the weight of a yoghurt cup, $X_{t,i,j}$, fits an AR(1) model with parameter $\phi = 0.38$, an IC mean estimate, $\mu_0 = 124.9g$ and an IC standard deviation, $\sigma_0 = 0.76g$. Moreover, an R&R study indicates that the measurement system standard deviation, $\sigma_M = 0.24g$, so that $\gamma$=0.316. For illustration purpose, assume the data in Table 10 is a full dataset and here we show how to implement the *s&m* sampling strategy to form rational subgroups of size *n*=3. In the last two columns, the corresponding plotting statistics at each sampling point for the 0&1 and 1&2 strategy are shown.

<Insert Table 10>

For instance, when $t$=1, these are calculated as follows:

$$\bar{X}_1 = \frac{1}{1\times 3}\left(X_{1,1,1} + X_{1,2,1} + X_{1,3,1}\right) = 125.33$$ – for the 0&1 strategy,

$\bar{X}_1 = \frac{1}{2\times 3}\left(X_{1,1,1} + X_{1,1,2} + X_{1,3,1} + X_{1,3,2} + X_{1,5,1} + X_{1,5,2}\right) = 124.82$ – for the 1&2 strategy.

The control limits parameters are calculated in Table 11 using Equation (7) for the steady-state RR4 or S4 *s&m* scheme and the corresponding monitoring schemes are constructed in Figure 2 when $s \in \{0,1\}$, $m \in \{1,2\}$ and these are compared to the basic $\bar{X}$ *s&m* scheme.

<Insert Table 11>

It is observed in Figure 2 that the RR4 or S4 scheme issues an OOC signal one sampling point earlier than each of the corresponding $\bar{X}$ scheme. That is, in Figure 2(a), the RR4 or S4 0&1 scheme issues an OOC signal for the first time at sampling point 13, whereas the $\bar{X}$ 0&1 scheme does so at sampling point 14. Similarly, in Figure 2(b), the RR4 or S4 1&2 scheme issues an OOC signal for the first time at sampling point 12, whereas the $\bar{X}$ 1&2 scheme does so at sampling point 13. This example illustrates the significance of increasing *s* and *m* to counteract the negative effect of autocorrelation and measurement errors. Visually, in Figure 2, it is observed that increasing *s* and *m* tend to have an improved detection rate because each of the monitoring schemes yields control limits that become narrower as *s* and *m* increase.

<Insert Figure 2>

**6. Conclusion remarks**

Since serial correlation and measurement inaccuracy are often encountered in real-life applications of SPM; then in this paper, the four design approaches of the 2-*of*-(*H*+1) runs-rules and synthetic schemes are considered in an effort to improve the classical Shewhart $\bar{X}$ scheme in the presence of both autocorrelation and measurement errors; however, focus is paid to the MSS design as it is shown to be the best performing design out of the other three. The first-order autoregressive model with *s*-skip sampling strategy and the additive model with *m*-multiple measurements sampling strategy are incorporated to the Markov chain matrix of the MSS runs-rules and synthetic schemes to reduce the negative effect of autocorrelation and measurement errors and are used to derive the zero- and steady-state run-length properties. Empirical analysis indicated that the zero-state MSS synthetic *s&m* scheme uniformly outperforms the $\bar{X}$ *s&m* scheme. However, the zero- and steady-state MSS runs-rules *s&m* scheme (as well as the steady-state MSS synthetic *s&m* scheme) outperforms the $\bar{X}$ *s&m* scheme for small to moderate shifts, the converse is true for large process shifts. Note though, using the *EARL* metric, both the MSS runs-rules and synthetic *s&m* schemes always yield a better zero- and steady-state performances than the $\bar{X}$ *s&m* scheme in all the corresponding cases.

Moreover, it has been observed that the autocorrelation level has a relatively higher negative effect than the level of measurement errors. A drawback of these new schemes is that, they require more observations (as some will be skipped during inspection) and more effort (multiple measurements on

each item are taken during inspection) as compared to the no remedy approach. Finally, we recommend that quality practitioners should implement any of the two proposed MSS schemes instead of the currently existing Shewhart $\bar{X}$ scheme when monitoring the process mean under the combined effect of measurement errors and autocorrelation.

**Acknowledgements**

We would like to convey our gratitude to the Editorial staff and the anonymous referee(s) who carefully read our earlier draft and gave us constructive comments to improve the paper.

**References**

Ahmad, S., M. Riaz, S. Hussain and S.A. Abbasi. 2019. On auxiliary information-based control charts for autocorrelated processes with application in manufacturing industry. *International Journal of Advanced Manufacturing Technology* 100 (5-8):1965-1980.

Alwan, L.C., and D. Radson. 1992. Time-series investigation of subsample mean chart. *IIE Transactions* 24 (5):66-80.

Antzoulakos, D.L., and A.C. Rakitzis. 2008. The modified *r* out of *m* control chart. *Communications in Statistics - Simulation and Computation* 37 (2):396-408.

Bourke, P.D. 1991. Detecting a shift in fraction nonconforming using run-length control charts with 100% inspection. *Journal of Quality Technology* 23 (3):225-238.

Box, G.E.P., G.M. Jenkins, and G.C. Reinsel. 2008. Time Series Analysis: Forecasting and Control, 4th ed. New York, NY: John Wiley & Sons.

Champ, C.W. 1992. Steady-state run length analysis of a Shewhart quality control chart with supplementary runs rules. *Communications in Statistics – Theory and Methods* 21 (3):765-777.

Chang, Y.-M., and T.-L. Wu. 2011. On average run lengths of control charts for autocorrelated processes. *Methodology and Computing in Applied Probability* 13 (2):419-431.

Claro, A.F.E., A.F.B. Costa, and M.A.G. Machado. 2008. Double sampling $\bar{X}$ control chart for a first order autoregressive process. *Pesquisa Operacional* 28 (3):545-562.

Costa, A.F.B., and P. Castagliola. 2011. Effect of measurement error and autocorrelation on the $\bar{X}$ chart. *Journal of Applied Statistics* 38 (4):661-673.

Costa, A.F.B., and M.A.G. Machado. 2011. Variable parameter and double sampling $\bar{X}$ charts in the presence of correlation: the Markov chain approach. *International Journal of Production Economics* 130 (2):224-229.

Dargopatil, P., and V. Ghute. 2019. New sampling strategies to reduce the effect of autocorrelation on the synthetic $T^2$ chart to monitor bivariate process. *Quality and Reliability Engineering International* 35 (1):30-46.

Davis, R.B., and W.H. Woodall. 2002. Evaluating and improving the synthetic control chart. *Journal of Quality Technology* 34 (2):200-208.

Derman, C., and S.M. Ross. 1997. *Statistical Aspects of Quality Control*. San Diego, CA: Academic Press.

Franco, B.C., P. Castagliola, G. Celano, A.F.B. Costa. 2014a. A new sampling strategy to reduce the effect of autocorrelation on a control chart. *Journal of Applied Statistics* 41 (7):1408-1421.

Franco, B.C., G. Celano, P. Castagliola, A.F.B. Costa. 2014b. Economic design of Shewhart control charts for monitoring autocorrelated data with skip sampling strategies. *International Journal of Production Economics* 151 (C):121-130.

Fu. J.C., and W.Y.W. Lou. 2003. *Distribution Theory of Runs and Patterns and Its Applications: A Finite Markov Chain Imbedding Approach.* Singapore: World Scientific Publishing.

Garza-Venegas, J.A., V.G. Tercero-Gómez, L. Lee-Ho, P. Castagliola, G. Celano. 2018. Effect of autocorrelation estimators on the performance of the $\bar{X}$ control chart. *Journal of Statistical Computation and Simulation* 88 (13):2612-2630.

Ghute, V.B., and D.T. Shirke. 2012. A nonparametric signed-rank control chart for bivariate process location. *Quality Technology & Quantitative Management* 9 (4):317-328.

Gilbert, K.C., K. Kirby, and C.R. Hild. 1993. Charting autocorrelated data: Guidelines for practitioner. *Quality Engineering* 9 (3):367-382.

Haq, A. 2019. A new nonparametric synthetic EWMA control chart for monitoring process mean. *Communications in Statistics – Simulation and Computation* 48 (6):1665-1676.

Haq, A., and M.B.C. Khoo. 2019. A synthetic double sampling control chart for process mean using auxiliary information, *Quality and Reliability Engineering International*; DOI: 10.1002/qre.2477.

Hu X.L., and J. Sun. 2015. Synthetic $\bar{X}$ chart for AR(1) autocorrelated processes. Proceedings of the 27th Chinese Control and Decision Conference (CCDC):7-12, DOI: 10.1109/CCDC.201527161658.

Kazemzadeh, R.B., R. Noorossana, and A. Amiri. 2010. Phase II monitoring of autocorrelated polynomial profiles in AR(1) processes. *Scientia Iranica* 17 (1):12-24.

Keramatpour, M., S.T.A. Niaki, and A. Amiri. 2014. Phase II monitoring of AR(1) autocorrelated polynomial profiles. *Journal of Optimization in Industrial Engineering* 14 (1):53-59.

Khaw, K.W., X. Chew, W.C. Yeong, and S.L. Lim. 2019. Optimal design of the synthetic control chart for monitoring the multivariate coefficient of variation. *Chemometrics and Intelligent Laboratory Systems* 186:33-40.

Khilare, S.K., and D.T. Shirke. 2010. A nonparametric synthetic control chart using sign statistic. *Communications in Statistics – Theory and Methods* 39 (18):3282-3293.

Khilare, S.K., and D.T. Shirke. 2012. Nonparametric synthetic control charts for process variation. *Quality and Reliability Engineering International* 28 (2):193-202.

Khilare, S.K., and D.T. Shirke. 2015. Steady-state behavior of nonparametric control charts using sign statistic. *Production* 25 (4):739-749.

Klein, M. 2000. Two alternatives to Shewhart $\bar{X}$ control chart. *Journal of Quality Technology* 32:427-431.

Leoni, R.C., A.F.B. Costa, B.C. Franco, and M.A.G. Machado. 2015a. The skipping strategy to reduce the effect of the autocorrelation on the $T^2$ chart's performance. *International Journal of Advanced Manufacturing Technology* 80 (9-12):1547-1559.

Leoni, R.C., A.F.B. Costa, and M.A.G. Machado. 2015b. The effect of the autocorrelation on the performance of the $T^2$ chart. *European Journal of Operational Research*, 247 (1):155-165.

Leoni, R.C., M.A.G. Machado, and A.F.B. Costa. 2015c. The $T^2$ chart with mixed samples to control bivariate autocorrelated processes. *International Journal of Production Research*, 54 (11):3294-3310.

Linna, K.W., and W.H. Woodall. 2001. Effect of measurement error on Shewhart control charts. *Journal of Quality Technology* 33 (2):213-222.

Machado, M.A.G., and A.F.B. Costa. 2014. Some comments regarding the synthetic chart. *Communications in Statistics - Theory and Methods* 43 (14):2897-2906.

Maleki, M.R., A. Amiri, and P. Castagliola. 2017. Measurement errors in statistical process monitoring: A literature review. *Computers & Industrial Engineering* 103:316-329.

Malela-Majika, J.-C., and E.M. Rapoo. 2017. Distribution-free synthetic and runs-rules control charts combined with a Mann-Whitney chart. *International Journal of Quality Engineering and Technology* 6 (4):219-248.

Malela-Majika, J.-C. 2019. Modified side-sensitive synthetic double sampling monitoring scheme for simultaneously monitoring the process mean and variability. *Computers and Industrial Engineering* 130:798-814.

Osei-Aning, R., S.A. Abbasi, and M. Riaz. 2017. Mixed EWMA-CUSUM and mixed CUSUM-EWMA for monitoring first order autoregressive processes. *Quality Technology & Quantitative Management* 14 (4):429-453.

Pawar, V.Y., D.T. Shirke, and S.K. Khilare. 2018. Steady-state behavior of nonparametric synthetic control chart using signed-rank statistic. *Pakistan Journal of Statistics & Operations Research* 14 (1):185-198.

Pawar, V.Y., and D.T. Shirke. 2010. A nonparametric Shewhart-type synthetic control chart. *Communications in Statistics – Theory and Methods* 39 (8):1493-1505.

Rakitzis, A.C., S. Chakraborti, S.C. Shongwe, M.A. Graham, M.B.C. Khoo. 2019. An overview of synthetic-type control charts: Techniques and Methodology. *Quality and Reliability Engineering International* DOI: 10.1002/qre.2491.

Raza, M.A., T. Nawaz, and D. Han. 2019. On designing new optimal synthetic Tukey's control charts. *Journal of Statistical Computation and Simulation* DOI: 10.1080/00949655.2019.1615062.

Reynolds Jr., M.R., and J. Lou. 2010. An evaluation of a GLR control chart for monitoring the process mean. *Journal of Quality Technology* 42 (3):287-310.

Ryu, J.-H., H. Wan, and S. Kim. 2010. Optimal design of a CUSUM chart for a mean shift of unknown size. *Journal of Quality Technology* 42 (3):311-326.

Sabahno, H., A. Amiri, P. Castagliola. 2019. Performance of the variable parameters $\bar{X}$ control chart in presence of measurement errors. *Journal of Testing and Evaluation* 47 (1):480-497.

Scagliarini, M. 2002. Estimation of $C_p$ for autocorrelated data and measurement errors. *Communications in Statistics-Theory and Methods* 31 (9):1647-1664.

Scagliarini, M. 2010. Inference on $C_{p^k}$ for autocorrelated data in the presence of random measurement errors. *Journal of Applied Statistics* 37 (1):147-158.

Shongwe, S.C., and M.A. Graham. 2018. A modified side-sensitive synthetic chart to monitor the process mean. *Quality Technology and Quantitative Management* 15 (3):328-353.

Shongwe, S.C., and M.A. Graham. 2019a. Some theoretical comments regarding the run-length properties of the synthetic and runs-rules monitoring schemes – Part 2: Steady-state. *Quality Technology & Quantitative Management* 16 (2):190-199.

Shongwe, S.C., and M.A. Graham. 2019b. Some theoretical comments regarding the run-length properties of the synthetic and runs-rules monitoring schemes – Part 1: Zero-state. *Quality Technology & Quantitative Management* 16 (2):170-189.

Shongwe, S.C., J.-C. Malela-Majika, P. Castagliola, and T. Molahloe. 2019a. Side-sensitive synthetic and runs-rules charts for monitoring AR(1) processes with skipping sampling strategies. *Communications in Statistics – Theory and Methods* DOI: 10.1080/03610926.2019.1596284.

Shongwe, S.C., J.-C. Malela-Majika, and T. Molahloe. 2019b. One-sided runs-rules schemes to monitor autocorrelated time series data using a first-order autoregressive model with skipping sampling strategies. *Quality and Reliability Engineering International* DOI: 10.1002/qre.2487.

Tang, A.A., P. Castagliola, X. Hu, and J. Sun. 2019. The performance of the adaptive EWMA median chart in the presence of measurement error. *Quality and Reliability Engineering International* 35 (1):423-438.

Tran, K.P., P. Castagliola, and N. Balakrishnan. 2017. On the performance of Shewhart median chart in the presence of measurement errors. *Quality and Reliability Engineering International* 33 (5):1019-1029.

Tran, P.H., K.P. Tran, and A.C. Rakitzis. 2019. A synthetic median control chart for monitoring the process mean with measurement errors. *Quality and Reliability Engineering International* 35 (4):1100-1116.

Wu, Z., and T.A. Spedding. 2000. A synthetic control chart for detecting small shifts in the process mean. *Journal of Quality Technology* 32 (1):32-38.

Wu, Z., W. Yang, W. Jian, and M.B.C. Khoo. 2008. Optimization designs of the combined Shewhart-CUSUM control charts. *Computational Statistics & Data Analysis* 53 (2):496-506.

Xiaohong, L., and W. Zhaojun. 2009. The CUSUM control chart for the autocorrelated data with measurement error. *Chinese Journal of Applied Probability* 25 (5):461-474.

Yang, S.F., and C.M. Yang. 2005. Effects of imprecise measurement on the two dependent processes control for the autocorrelated observations. *International Journal of Advanced Manufacturing Technology* 26 (5-6):623-630.

Yeong, W.C., M.B.C. Khoo, S.L. Lim, and W.L. Teoh. 2017. The coefficient of variation chart with measurement error. *Quality Technology & Quantitative Management* 14 (4):353-377.

You, H.W. 2017. Run length distribution of synthetic double sampling chart. *International Journal of Applied Engineering* 12 (24):14268-14272.

You, H.W. 2018. Performance of the synthetic double sampling chart with estimated parameters based on expected average run length. *Journal of Probability and Statistics* Article ID 7583610, 6 pages.

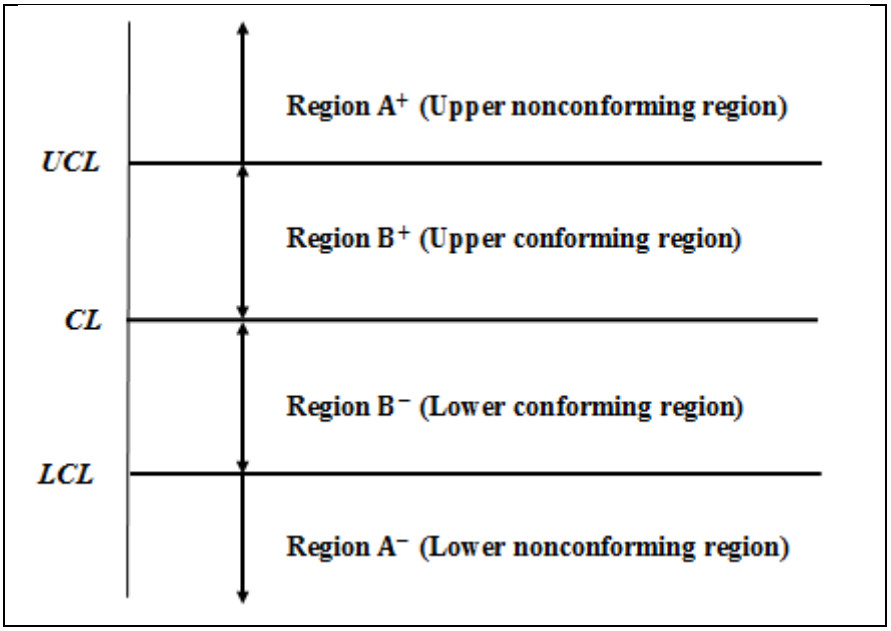


**Figure 1:** Charting regions and limits for the $\bar{X}$ sub-chart

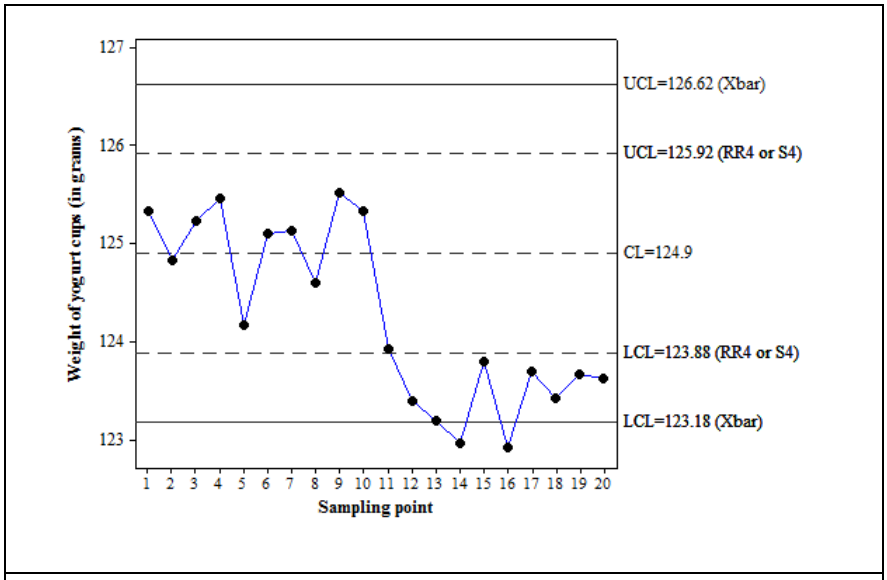


(a) $s$=0 & $m$=1

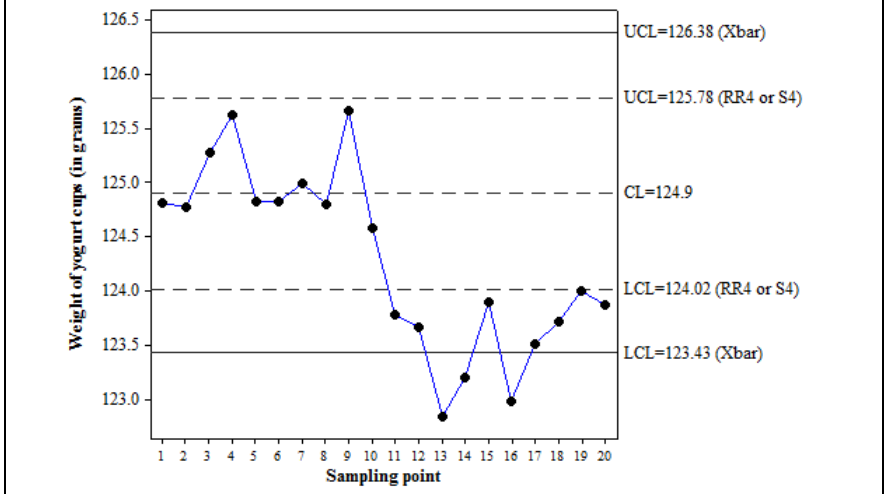


(b) $s$=1 & $m$=2

**Figure 2:** The weight of the yoghurt cups example using the RR4 / S4 and the basic $\bar{X}$ schemes with *s&m* sampling strategy

**Table 1:** Operation of the MSS runs-rules and synthetic *s&m* schemes

| Step | Methodology |
|---|---|
| 1 | Specify $H$, $\phi$, $\gamma$, $n$, $m$, $s$ and $ARL_0$. Numerically search for the corresponding value of $k$ such that the attained IC $ARL$ (expression derived in Section 3.3) is equal to $ARL_0$. |
| 2 | Compute $UCL$ / $CL$ / $LCL$ using Equations (7) and (8). |
| 3 | At each inspection point, implement the *s&m* sampling strategy to collect a sample of size $n$ and calculate $\bar{X}_t$. |
| 4 | If $\bar{X}_t \in$ Region $B^+$ or $B^-$, return to Step 3; otherwise, go to Step 5. |
| 5 | If $\bar{X}_t \in$ Region $A^+$, go to Step 6a; otherwise, if $\bar{X}_t \in A^-$, go to Step 6b. |
| 6 | **(a)** Calculate $CRL^+$ and if $CRL^+ \leq H$ go to Step 7; otherwise return to Step 3.<br>**(b)** Calculate $CRL^-$ and if $CRL^- \leq H$ go to Step 7; otherwise return to Step 3. |
| 7 | Issue an OOC signal. Take necessary corrective action to find and remove the assignable causes and return to Step 3. |

**Table 2:** General form of the TPM for the MSS synthetic scheme (and MSS runs-rules scheme - by removing the head-start feature elements)

| | $\eta_1$ | $\eta_2$ | $\cdots$ | $\eta_{l-3}$ | $\eta_{l-2}$ | $\eta_{l-1}$ | $\varphi$ | $\eta_{l+1}$ | $\eta_{l+2}$ | $\eta_{l+3}$ | $\cdots$ | $\eta_{\tau-2}$ | $\eta_{\tau-1}$ | $\eta_\tau$ | $\boldsymbol{\psi_1}$ | $\boldsymbol{\psi_2}$ | $\boldsymbol{\psi_3}$ | $\boldsymbol{\psi_4}$ | $\boldsymbol{\psi_5}$ | $\cdots$ | $\boldsymbol{\psi_{\kappa-3}}$ | $\boldsymbol{\psi_{\kappa-2}}$ | $\boldsymbol{\psi_{\kappa-1}}$ | $\boldsymbol{\psi_\kappa}$ | OOC |
|---|---|---|---|---|---|---|---|---|---|---|---|---|---|---|---|---|---|---|---|---|---|---|---|---|---|
| $\eta_1$ | | | | | | | $p_{B^+}+p_{B^-}$ | $p_{A^-}$ | | | | | | | | | | | | | | | | | $p_{A^+}$ |
| $\eta_2$ | $p_{B^+}$ | | | | | | $p_{B^-}$ | $p_{A^-}$ | | | | | | | | | | | | | | | | | $p_{A^+}$ |
| $\eta_3$ | | $p_{B^+}$ | | | | | $p_{B^-}$ | $p_{A^-}$ | | | | | | | | | | | | | | | | | $p_{A^+}$ |
| $\vdots$ | | | $\ddots$ | | | | $\vdots$ | $\vdots$ | | | | | | | | | | | | | | | | | $\vdots$ |
| $\eta_{l-2}$ | | | | $p_{B^+}$ | | | $p_{B^-}$ | $p_{A^-}$ | | | | | | | | | | | | | | | | | $p_{A^+}$ |
| $\eta_{l-1}$ | | | | | $p_{B^+}$ | | $p_{B^-}$ | $p_{A^-}$ | | | | | | | | | | | | | | | | | $p_{A^+}$ |
| $\varphi$ | | | | | | $p_{A^+}$ | $p_{B^+}+p_{B^-}$ | $p_{A^-}$ | | | | | | | | | | | | | | | | | |
| $\eta_{l+1}$ | | | | | | $p_{A^+}$ | $p_{B^+}$ | | $p_{B^-}$ | | | | | | | | | | | | | | | | $p_{A^-}$ |
| $\eta_{l+2}$ | | | | | | $p_{A^+}$ | $p_{B^+}$ | | | $p_{B^-}$ | | | | | | | | | | | | | | | $p_{A^-}$ |
| $\vdots$ | | | | | | $\vdots$ | $\vdots$ | | | | $\ddots$ | | | | | | | | | | | | | | $\vdots$ |
| $\eta_{\tau-3}$ | | | | | | $p_{A^+}$ | $p_{B^+}$ | | | | | $p_{B^-}$ | | | | | | | | | | | | | $p_{A^-}$ |
| $\eta_{\tau-2}$ | | | | | | $p_{A^+}$ | $p_{B^+}$ | | | | | | $p_{B^-}$ | | | | | | | | | | | | $p_{A^-}$ |
| $\eta_{\tau-1}$ | | | | | | $p_{A^+}$ | $p_{B^+}$ | | | | | | | $p_{B^-}$ | | | | | | | | | | | $p_{A^-}$ |
| $\eta_\tau$ | | | | | | $p_{A^+}$ | $p_{B^+}+p_{B^-}$ | | | | | | | | | | | | | | | | | | $p_{A^-}$ |
| $\boldsymbol{\psi_1}$ | | | | | | | | | | | | | | | $p_{B^+}$ | $p_{B^-}$ | | | | | | | | | $p_{A^+}+p_{A^-}$ |
| $\boldsymbol{\psi_2}$ | | | | | | | $p_{B^-}$ | $p_{A^-}$ | | | | | | | | | $p_{B^+}$ | | | | | | | | $p_{A^+}$ |
| $\boldsymbol{\psi_3}$ | | | | | | $p_{A^+}$ | $p_{B^+}$ | | | | | | | | | | | $p_{B^-}$ | | | | | | | $p_{A^-}$ |
| $\vdots$ | | | | | | $\vdots$ | $\vdots$ | | | | | | | | | | | | $\ddots$ | | | | | | $\vdots$ |
| $\boldsymbol{\psi_{\kappa-5}}$ | | | | | | | $p_{B^-}$ | $p_{A^-}$ | | | | | | | | | | | | $p_{B^+}$ | | | | | $p_{A^+}$ |
| $\boldsymbol{\psi_{\kappa-4}}$ | | | | | | $p_{A^+}$ | $p_{B^+}$ | | | | | | | | | | | | | | $p_{B^-}$ | | | | $p_{A^-}$ |
| $\boldsymbol{\psi_{\kappa-3}}$ | | | | | | | $p_{B^-}$ | $p_{A^-}$ | | | | | | | | | | | | | | $p_{B^+}$ | | | $p_{A^+}$ |
| $\boldsymbol{\psi_{\kappa-2}}$ | | | | | | $p_{A^+}$ | $p_{B^+}$ | | | | | | | | | | | | | | | | $p_{B^-}$ | | $p_{A^-}$ |
| $\boldsymbol{\psi_{\kappa-1}}$ | | | | | | | $p_{B^+}+p_{B^-}$ | $p_{A^-}$ | | | | | | | | | | | | | | | | | $p_{A^+}$ |
| $\boldsymbol{\psi_\kappa}$ | | | | | | $p_{A^+}$ | $p_{B^+}+p_{B^-}$ | | | | | | | | | | | | | | | | | | $p_{A^-}$ |
| OOC | | | | | | | | | | | | | | | | | | | | | | | | | 1 |

**Table 3:** The zero- and steady-state design parameters $H$ and $k$ of the RR4 and S4 schemes for $H \in \{1,2,3,\ldots,20,50,100\}$ for $ARL_0$=370.4

| | **Zero-state** | | **Steady-state** |
|---|---|---|---|
| ***H*** | **RR4** | **S4** | **RR4 & S4** |
| 1 | 1.7814 | 1.7982 | 1.7820 |
| 2 | 1.8664 | 1.8862 | 1.8671 |
| 3 | 1.8969 | 1.9181 | 1.8978 |
| 4 | 1.9099 | 1.9318 | 1.9109 |
| 5 | 1.9158 | 1.9380 | 1.9168 |
| 6 | 1.9186 | 1.9409 | 1.9197 |
| 7 | 1.9199 | 1.9422 | 1.9210 |
| 8 | 1.9205 | 1.9429 | 1.9216 |
| 9 | 1.9208 | 1.9432 | 1.9219 |
| 10 | 1.9209 | 1.9433 | 1.9220 |
| 11 | **1.9210** | 1.9434 | **1.9221** |
| 12 | **1.9210** | **1.9435** | **1.9221** |
| 13 | **1.9210** | **1.9435** | **1.9221** |
| 14 | **1.9210** | **1.9435** | **1.9221** |
| 15 | **1.9210** | **1.9435** | **1.9221** |
| 16 | **1.9210** | **1.9435** | **1.9221** |
| 17 | **1.9210** | **1.9435** | **1.9221** |
| 18 | **1.9210** | **1.9435** | **1.9221** |
| 19 | **1.9210** | **1.9435** | **1.9221** |
| 20 | **1.9210** | **1.9435** | **1.9221** |
| ⋮ | ⋮ | ⋮ | ⋮ |
| 50 | **1.9210** | **1.9435** | **1.9221** |
| ⋮ | ⋮ | ⋮ | ⋮ |
| 100 | **1.9210** | **1.9435** | **1.9221** |

**Table 4:** The zero-state (ZS) and steady-state (SS) *ARL*, *EARL* and *PCI* when $\phi \in \{0,0.5\}$, $\gamma \in \{0,0.5\}$, $H$=7, $n$=5, $s$=0, $m$=1, $\delta_{min}$=0, $\delta_{max}$= 3 and $ARL_0$=370.4 for the basic $\bar{X}$, RR4 and S4 schemes

| | $(\phi,\gamma)$ | (0,0) | | | | (0,0.5) | | | | (0.5,0) | | | | (0.5,0.5) | | | |
|---|---|---|---|---|---|---|---|---|---|---|---|---|---|---|---|---|---|
| | Mode | | SS | ZS | ZS | | SS | ZS | ZS | | SS | ZS | ZS | | SS | ZS | ZS |
| | Scheme | $\bar{X}$ | RR4&S4 | RR4 | S4 | $\bar{X}$ | RR4&S4 | RR4 | S4 | $\bar{X}$ | RR4&S4 | RR4 | S4 | $\bar{X}$ | RR4&S4 | RR4 | S4 |
| $\delta$ | 0 | 370.4 | 370.4 | 370.4 | 370.4 | 370.4 | 370.4 | 370.4 | 370.4 | 370.4 | 370.4 | 370.4 | 370.4 | 370.4 | 370.4 | 370.4 | 370.4 |
| | 0.25 | 133.2 | 62.7 | 63.0 | 54.9 | 155.2 | 78.0 | 78.3 | 69.9 | 212.8 | 126.7 | 127.1 | 118.7 | 223.0 | 136.9 | 137.2 | 128.9 |
| | 0.5 | 33.4 | 12.7 | 12.8 | 8.5 | 43.9 | 16.6 | 16.8 | 11.7 | 81.3 | 33.0 | 33.3 | 26.5 | 89.8 | 37.3 | 37.6 | 30.5 |
| | 0.75 | 10.8 | 5.2 | 5.3 | 2.9 | 15.0 | 6.5 | 6.6 | 3.8 | 32.9 | 12.5 | 12.7 | 8.3 | 37.6 | 14.2 | 14.4 | 9.7 |
| | 1 | 4.5 | 3.2 | 3.2 | 1.7 | 6.3 | 3.8 | 3.8 | 2.0 | 15.0 | 6.5 | 6.6 | 3.8 | 17.5 | 7.3 | 7.4 | 4.3 |
| | 1.25 | 2.4 | 2.4 | 2.5 | 1.2 | 3.2 | 2.7 | 2.8 | 1.4 | 7.7 | 4.2 | 4.3 | 2.3 | 9.0 | 4.6 | 4.7 | 2.5 |
| | 1.5 | 1.6 | 2.1 | 2.2 | 1.1 | 2.0 | 2.3 | 2.3 | 1.2 | 4.4 | 3.1 | 3.2 | 1.6 | 5.2 | 3.4 | 3.5 | 1.8 |
| | 1.75 | 1.2 | 2.0 | 2.0 | 1.0 | 1.5 | 2.1 | 2.1 | 1.1 | 2.8 | 2.6 | 2.6 | 1.3 | 3.3 | 2.7 | 2.8 | 1.4 |
| | 2 | 1.1 | 2.0 | 2.0 | 1.0 | 1.2 | 2.0 | 2.0 | 1.0 | 2.0 | 2.3 | 2.3 | 1.2 | 2.3 | 2.4 | 2.4 | 1.2 |
| | 2.25 | 1.0 | 2.0 | 2.0 | 1.0 | 1.1 | 2.0 | 2.0 | 1.0 | 1.6 | 2.1 | 2.2 | 1.1 | 1.7 | 2.2 | 2.2 | 1.1 |
| | 2.5 | 1.0 | 2.0 | 2.0 | 1.0 | 1.0 | 2.0 | 2.0 | 1.0 | 1.3 | 2.0 | 2.1 | 1.0 | 1.4 | 2.1 | 2.1 | 1.1 |
| | 2.75 | 1.0 | 2.0 | 2.0 | 1.0 | 1.0 | 2.0 | 2.0 | 1.0 | 1.2 | 2.0 | 2.0 | 1.0 | 1.2 | 2.0 | 2.0 | 1.0 |
| | 3 | 1.0 | 2.0 | 2.0 | 1.0 | 1.0 | 2.0 | 2.0 | 1.0 | 1.1 | 2.0 | 2.0 | 1.0 | 1.1 | 2.0 | 2.0 | 1.0 |
| | *EARL* | 187.5 | 156.9 | 157.1 | 148.9 | 200.9 | 164.1 | 164.4 | 155.5 | 244.8 | 189.8 | 190.3 | 179.4 | 254.5 | 195.8 | 196.2 | 185.0 |
| | *PCI* | 1.00 | 0.84 | 0.84 | 0.79 | 1.00 | 0.82 | 0.82 | 0.77 | 1.00 | 0.78 | 0.78 | 0.73 | 1.00 | 0.77 | 0.77 | 0.73 |

**Table 5:** The zero-state *ARL* and *EARL* of the S4 scheme when $\phi$=0.5, $\gamma$=0.5, $n$=5, $H\in\{1,2,3,\ldots,11,12\}$, $s\&m\in\{0\&1, 3\&4\}$, $\delta_{min}$=0, $\delta_{max}$=3 and $ARL_0$=370.4

| | | ***H*** | | | | | | | | | | | | | | | | | | | | | |
|---|---|---|---|---|---|---|---|---|---|---|---|---|---|---|---|---|---|---|---|---|---|---|---|
| | | **1** | | **2** | | **3** | | **4** | | **5** | | **6** | | **7** | | **8** | | **9** | | **10** | | **11** | | **12** | |
| | | **0&1** | **3&4** | **0&1** | **3&4** | **0&1** | **3&4** | **0&1** | **3&4** | **0&1** | **3&4** | **0&1** | **3&4** | **0&1** | **3&4** | **0&1** | **3&4** | **0&1** | **3&4** | **0&1** | **3&4** | **0&1** | **3&4** | **0&1** | **3&4** |
| | **0** | 370.4 | 370.4 | 370.4 | 370.4 | 370.4 | 370.4 | 370.4 | 370.4 | 370.4 | 370.4 | 370.4 | 370.4 | 370.4 | 370.4 | 370.4 | 370.4 | 370.4 | 370.4 | 370.4 | 370.4 | 370.4 | 370.4 | 370.4 | 370.4 |
| | **0.25** | 169.2 | 97.5 | 151.9 | 83.1 | 142.4 | 75.5 | 136.5 | 71.0 | 132.8 | 68.1 | 130.4 | 66.2 | 128.9 | 65.1 | 128.1 | 64.3 | 127.5 | 63.8 | 127.2 | 63.5 | 127.0 | 63.4 | 126.9 | 63.2 |
| | **0.5** | 51.7 | 20.1 | 42.0 | 15.5 | 37.2 | 13.4 | 34.3 | 12.2 | 32.5 | 11.4 | 31.3 | 10.9 | 30.5 | 10.6 | 30.1 | 10.4 | 29.7 | 10.3 | 29.5 | 10.2 | 29.4 | 10.1 | 29.3 | 10.1 |
| | **0.75** | 18.5 | 6.2 | 14.2 | 4.7 | 12.3 | 4.1 | 11.1 | 3.8 | 10.5 | 3.6 | 10.0 | 3.5 | 9.7 | 3.5 | 9.6 | 3.4 | 9.4 | 3.4 | 9.4 | 3.4 | 9.3 | 3.4 | 9.3 | 3.4 |
| | **1** | 8.0 | 2.7 | 6.1 | 2.2 | 5.2 | 2.0 | 4.8 | 1.9 | 4.6 | 1.9 | 4.4 | 1.9 | 4.3 | 1.9 | 4.3 | 1.9 | 4.2 | 1.9 | 4.2 | 1.9 | 4.2 | 1.9 | 4.2 | 1.9 |
| | **1.25** | 4.1 | 1.6 | 3.2 | 1.4 | 2.8 | 1.4 | 2.7 | 1.4 | 2.6 | 1.4 | 2.6 | 1.4 | 2.5 | 1.4 | 2.5 | 1.4 | 2.5 | 1.4 | 2.5 | 1.4 | 2.5 | 1.4 | 2.5 | 1.4 |
| ***δ*** | **1.5** | 2.5 | 1.2 | 2.0 | 1.1 | 1.9 | 1.1 | 1.8 | 1.1 | 1.8 | 1.1 | 1.8 | 1.1 | 1.8 | 1.1 | 1.8 | 1.1 | 1.8 | 1.1 | 1.8 | 1.1 | 1.8 | 1.1 | 1.8 | 1.1 |
| | **1.75** | 1.8 | 1.1 | 1.5 | 1.0 | 1.4 | 1.0 | 1.4 | 1.0 | 1.4 | 1.0 | 1.4 | 1.0 | 1.4 | 1.0 | 1.4 | 1.0 | 1.4 | 1.0 | 1.4 | 1.0 | 1.4 | 1.0 | 1.4 | 1.0 |
| | **2** | 1.4 | 1.0 | 1.2 | 1.0 | 1.2 | 1.0 | 1.2 | 1.0 | 1.2 | 1.0 | 1.2 | 1.0 | 1.2 | 1.0 | 1.2 | 1.0 | 1.2 | 1.0 | 1.2 | 1.0 | 1.2 | 1.0 | 1.2 | 1.0 |
| | **2.25** | 1.2 | 1.0 | 1.1 | 1.0 | 1.1 | 1.0 | 1.1 | 1.0 | 1.1 | 1.0 | 1.1 | 1.0 | 1.1 | 1.0 | 1.1 | 1.0 | 1.1 | 1.0 | 1.1 | 1.0 | 1.1 | 1.0 | 1.1 | 1.0 |
| | **2.5** | 1.1 | 1.0 | 1.1 | 1.0 | 1.1 | 1.0 | 1.1 | 1.0 | 1.1 | 1.0 | 1.1 | 1.0 | 1.1 | 1.0 | 1.1 | 1.0 | 1.1 | 1.0 | 1.1 | 1.0 | 1.1 | 1.0 | 1.1 | 1.0 |
| | **2.75** | 1.0 | 1.0 | 1.0 | 1.0 | 1.0 | 1.0 | 1.0 | 1.0 | 1.0 | 1.0 | 1.0 | 1.0 | 1.0 | 1.0 | 1.0 | 1.0 | 1.0 | 1.0 | 1.0 | 1.0 | 1.0 | 1.0 | 1.0 | 1.0 |
| | **3** | 1.0 | 1.0 | 1.0 | 1.0 | 1.0 | 1.0 | 1.0 | 1.0 | 1.0 | 1.0 | 1.0 | 1.0 | 1.0 | 1.0 | 1.0 | 1.0 | 1.0 | 1.0 | 1.0 | 1.0 | 1.0 | 1.0 | 1.0 | 1.0 |
| **EARL** | | **210.6** | **168.6** | **198.9** | **161.5** | **193.0** | **158.0** | **189.5** | **155.9** | **187.3** | **154.6** | **185.9** | **153.8** | **185.0** | **153.3** | **184.5** | **153.0** | **184.1** | **152.8** | **183.9** | **152.6** | **183.8** | **152.6** | **183.7** | **152.5** |
| **%Diff** | | 24.9% | | 23.2% | | 22.2% | | 21.5% | | 21.1% | | 20.9% | | 20.6% | | 20.6% | | 20.5% | | 20.5% | | 20.5% | | 20.5% | |
| **OPG(H)** | | N/A | N/A | 5.9% | 4.4% | 3.1% | 2.2% | 1.9% | 1.3% | 1.1% | 0.8% | 0.8% | 0.5% | 0.5% | 0.3% | 0.2% | 0.2% | 0.2% | 0.1% | 0.1% | 0.1% | 0.1% | 0.0% | 0.0% | 0.0% |

**Table 6:** The steady-state *ARL* and *EARL* of the RR4 and S4 schemes when $\phi$=0.5, $\gamma$=0.5, $n$=5, $H\in\{1,2,3,\ldots,11,12\}$, $s\&m\in\{0\&1, 3\&4\}$, $\delta_{min}$=0, $\delta_{max}$=3 and $ARL_0$=370.4

| | | ***H*** | | | | | | | | | | | | | | | | | | | | | |
|---|---|---|---|---|---|---|---|---|---|---|---|---|---|---|---|---|---|---|---|---|---|---|---|
| | | **1** | | **2** | | **3** | | **4** | | **5** | | **6** | | **7** | | **8** | | **9** | | **10** | | **11** | | **12** | |
| | | **0&1** | **3&4** | **0&1** | **3&4** | **0&1** | **3&4** | **0&1** | **3&4** | **0&1** | **3&4** | **0&1** | **3&4** | **0&1** | **3&4** | **0&1** | **3&4** | **0&1** | **3&4** | **0&1** | **3&4** | **0&1** | **3&4** | **0&1** | **3&4** |
| | **0** | 370.4 | 370.4 | 370.4 | 370.4 | 370.4 | 370.4 | 370.4 | 370.4 | 370.4 | 370.4 | 370.4 | 370.4 | 370.4 | 370.4 | 370.4 | 370.4 | 370.4 | 370.4 | 370.4 | 370.4 | 370.4 | 370.4 | 370.4 | 370.4 |
| | **0.25** | 173.6 | 102.4 | 157.7 | 89.3 | 149.1 | 82.5 | 143.8 | 78.4 | 140.3 | 75.8 | 138.2 | 74.1 | 136.9 | 73.1 | 136.1 | 72.4 | 135.6 | 71.9 | 135.2 | 71.6 | 135.1 | 71.5 | 134.9 | 71.3 |
| | **0.5** | 56.2 | 23.6 | 47.6 | 19.5 | 43.3 | 17.7 | 40.7 | 16.6 | 39.1 | 16.0 | 38.0 | 15.6 | 37.4 | 15.3 | 36.9 | 15.1 | 36.6 | 15.0 | 36.4 | 14.9 | 36.2 | 14.8 | 36.2 | 14.8 |
| | **0.75** | 21.9 | 8.3 | 18.1 | 7.1 | 16.4 | 6.6 | 15.5 | 6.3 | 14.9 | 6.2 | 14.5 | 6.1 | 14.2 | 6.0 | 14.0 | 6.0 | 13.9 | 6.0 | 13.9 | 6.0 | 13.8 | 6.0 | 13.8 | 6.0 |
| | **1** | 10.4 | 4.2 | 8.8 | 3.8 | 8.1 | 3.6 | 7.7 | 3.6 | 7.5 | 3.6 | 7.4 | 3.6 | 7.3 | 3.6 | 7.2 | 3.6 | 7.2 | 3.6 | 7.2 | 3.6 | 7.2 | 3.6 | 7.2 | 3.6 |
| | **1.25** | 6.0 | 2.8 | 5.2 | 2.6 | 4.9 | 2.6 | 4.8 | 2.6 | 4.7 | 2.6 | 4.7 | 2.6 | 4.6 | 2.6 | 4.6 | 2.6 | 4.6 | 2.6 | 4.6 | 2.6 | 4.6 | 2.6 | 4.6 | 2.6 |
| ***δ*** | **1.5** | 4.0 | 2.3 | 3.6 | 2.2 | 3.5 | 2.2 | 3.4 | 2.2 | 3.4 | 2.2 | 3.4 | 2.2 | 3.4 | 2.2 | 3.4 | 2.2 | 3.4 | 2.2 | 3.4 | 2.2 | 3.4 | 2.2 | 3.4 | 2.2 |
| | **1.75** | 3.0 | 2.1 | 2.8 | 2.0 | 2.7 | 2.0 | 2.7 | 2.0 | 2.7 | 2.0 | 2.7 | 2.0 | 2.7 | 2.0 | 2.7 | 2.0 | 2.7 | 2.0 | 2.7 | 2.0 | 2.7 | 2.0 | 2.7 | 2.0 |
| | **2** | 2.5 | 2.0 | 2.4 | 2.0 | 2.4 | 2.0 | 2.4 | 2.0 | 2.4 | 2.0 | 2.4 | 2.0 | 2.4 | 2.0 | 2.4 | 2.0 | 2.4 | 2.0 | 2.4 | 2.0 | 2.4 | 2.0 | 2.4 | 2.0 |
| | **2.25** | 2.2 | 2.0 | 2.2 | 2.0 | 2.2 | 2.0 | 2.2 | 2.0 | 2.2 | 2.0 | 2.2 | 2.0 | 2.2 | 2.0 | 2.2 | 2.0 | 2.2 | 2.0 | 2.2 | 2.0 | 2.2 | 2.0 | 2.2 | 2.0 |
| | **2.5** | 2.1 | 2.0 | 2.1 | 2.0 | 2.1 | 2.0 | 2.1 | 2.0 | 2.1 | 2.0 | 2.1 | 2.0 | 2.1 | 2.0 | 2.1 | 2.0 | 2.1 | 2.0 | 2.1 | 2.0 | 2.1 | 2.0 | 2.1 | 2.0 |
| | **2.75** | 2.0 | 2.0 | 2.0 | 2.0 | 2.0 | 2.0 | 2.0 | 2.0 | 2.0 | 2.0 | 2.0 | 2.0 | 2.0 | 2.0 | 2.0 | 2.0 | 2.0 | 2.0 | 2.0 | 2.0 | 2.0 | 2.0 | 2.0 | 2.0 |
| | **3** | 2.0 | 2.0 | 2.0 | 2.0 | 2.0 | 2.0 | 2.0 | 2.0 | 2.0 | 2.0 | 2.0 | 2.0 | 2.0 | 2.0 | 2.0 | 2.0 | 2.0 | 2.0 | 2.0 | 2.0 | 2.0 | 2.0 | 2.0 | 2.0 |
| **EARL** | | **218.8** | **175.4** | **208.3** | **169.0** | **203.0** | **165.9** | **199.9** | **164.0** | **197.9** | **162.9** | **196.7** | **162.2** | **195.9** | **161.7** | **195.3** | **161.4** | **195.0** | **161.2** | **194.8** | **161.1** | **194.7** | **161.0** | **194.6** | **161.0** |
| **%Diff** | | 24.7% | | 23.3% | | 22.4% | | 21.9% | | 21.5% | | 21.2% | | 21.1% | | 21.0% | | 21.0% | | 20.9% | | 20.9% | | 20.9% | |
| **OPG(H)** | | N/A | N/A | 5.0% | 3.8% | 2.6% | 1.9% | 1.6% | 1.1% | 1.0% | 0.7% | 0.6% | 0.5% | 0.4% | 0.3% | 0.3% | 0.2% | 0.2% | 0.1% | 0.1% | 0.1% | 0.1% | 0.0% | 0.0% | 0.0% |

**Table 7:** The steady-state *EARL* (and *OPG* - in brackets) of the RR4 and S4 *s&m* schemes when $H$=5, $\phi$=0.5, $n$=5, $\delta_{min}$=0, $\delta_{max}$=3, $m \in \{1,2,3,4\}$, $s \in \{0,1,2,3\}$, $\gamma \in \{0,0.1,0.2,\ldots,0.9\}$ and $ARL_0$=370.4

| | | $\gamma$ | | | | | | | | | |
|---|---|---|---|---|---|---|---|---|---|---|---|
| | $m$ | 0 | 0.1 | 0.2 | 0.3 | 0.4 | 0.5 | 0.6 | 0.7 | 0.8 | 0.9 |
| $s$=0 | 1 | 191.8 | 192.0 | 192.7 | 193.9 | 195.7 | 197.9 | 200.5 | 203.6 | 207.0 | 210.8 |
| | 2 | 191.8 (0%) | 191.9 (0.1%) | 192.3 (0.2%) | 192.9 (0.6%) | 193.7 (1.0%) | 194.9 (1.5%) | 196.2 (2.2%) | 197.8 (2.9%) | 199.6 (3.7%) | 201.6 (4.6%) |
| | 3 | 191.8 (0%) | 191.9 (0.0%) | 192.1 (0.1%) | 192.5 (0.2%) | 193.0 (0.3%) | 193.8 (0.6%) | 194.8 (0.7%) | 195.7 (1.1%) | 197.0 (1.3%) | 198.4 (1.6%) |
| | 4 | 191.8 (0%) | 191.9 (0.0%) | 192.0 (0.1%) | 192.3 (0.1%) | 192.7 (0.2%) | 193.3 (0.2%) | 193.9 (0.4%) | 194.8 (0.5%) | 195.7 (0.7%) | 196.8 (0.8%) |
| $s$=1 | 1 | 172.2 | 172.6 | 173.3 | 174.8 | 176.7 | 179.1 | 182.1 | 185.5 | 189.3 | 193.6 |
| | 2 | 172.2 (0%) | 172.4 (0.1%) | 172.8 (0.3%) | 173.5 (0.7%) | 174.5 (1.2%) | 175.7 (1.9%) | 177.2 (2.7%) | 179.0 (3.7%) | 181.0 (4.6%) | 183.3 (5.6%) |
| | 3 | 172.2 (0%) | 172.3 (0.0%) | 172.6 (0.1%) | 173.1 (0.3%) | 173.7 (0.5%) | 174.6 (0.6%) | 175.6 (0.9%) | 176.8 (1.2%) | 178.1 (1.6%) | 179.7 (2.0%) |
| | 4 | 172.2 (0%) | 172.3 (0.0%) | 172.6 (0.0%) | 172.9 (0.1%) | 173.3 (0.2%) | 174.0 (0.3%) | 174.8 (0.5%) | 175.7 (0.6%) | 176.7 (0.8%) | 177.9 (1.0%) |
| $s$=2 | 1 | 164.5 | 164.8 | 165.7 | 167.1 | 169.1 | 171.7 | 174.8 | 178.3 | 182.3 | 186.8 |
| | 2 | 164.5 (0%) | 164.7 (0.1%) | 165.1 (0.3%) | 165.8 (0.8%) | 166.8 (1.4%) | 168.1 (2.1%) | 169.7 (3.0%) | 171.6 (3.9%) | 173.6 (5.0%) | 176.0 (6.1%) |
| | 3 | 164.5 (0%) | 164.6 (0.0%) | 164.9 (0.1%) | 165.4 (0.2%) | 166.1 (0.5%) | 166.9 (0.7%) | 167.9 (1.1%) | 169.2 (1.4%) | 170.7 (1.7%) | 172.3 (2.2%) |
| | 4 | 164.5 (0%) | 164.6 (0.0%) | 164.8 (0.1%) | 165.2 (0.1%) | 165.7 (0.2%) | 166.4 (0.3%) | 167.1 (0.5%) | 168.1 (0.7%) | 169.1 (0.9%) | 170.3 (1.2%) |
| $s$=3 | 1 | 161.0 | 161.4 | 162.3 | 163.7 | 165.8 | 168.4 | 171.6 | 175.2 | 179.3 | 183.8 |
| | 2 | 161.0 (0%) | 161.2 (0.1%) | 161.7 (0.4%) | 162.4 (0.8%) | 163.4 (1.4%) | 164.8 (2.2%) | 166.4 (3.1%) | 168.3 (4.1%) | 170.4 (5.2%) | 172.8 (6.3%) |
| | 3 | 161.0 (0%) | 161.2 (0.0%) | 161.5 (0.1%) | 162.0 (0.3%) | 162.6 (0.5%) | 163.5 (0.8%) | 164.7 (1.1%) | 165.9 (1.4%) | 167.3 (1.8%) | 169.0 (2.3%) |
| | 4 | 161.0 (0%) | 161.1 (0.0%) | 161.4 (0.1%) | 161.8 (0.1%) | 162.3 (0.2%) | 162.9 (0.3%) | 163.7 (0.6%) | 164.7 (0.7%) | 165.8 (0.9%) | 167.0 (1.2%) |

**Table 8:** The steady-state *EARL* (and *OPG* - in brackets) of the RR4 and S4 *s&m* schemes when $H$=5, $\gamma$=0.5, $n$=5, $\delta_{min}$=0, $\delta_{max}$=3, $m \in \{1,2,3,4\}$, $s \in \{0,1,2,3\}$, $\phi \in \{0,0.1,0.2,\ldots,0.9\}$ and $ARL_0$=370.4

| | | $\phi$ | | | | | | | | | |
|---|---|---|---|---|---|---|---|---|---|---|---|
| | $s$ | 0 | 0.1 | 0.2 | 0.3 | 0.4 | 0.5 | 0.6 | 0.7 | 0.8 | 0.9 |
| $m$=1 | 0 | 165.4 | 170.3 | 176.0 | 182.4 | 189.7 | 197.9 | 207.0 | 217.2 | 228.5 | 240.7 |
| | 1 | 165.4 (0%) | 165.9 (2.7%) | 167.3 (5.2%) | 169.8 (7.4%) | 173.6 (9.3%) | 179.1 (10.5%) | 186.7 (10.9%) | 197.1 (10.2%) | 211.0 (8.3%) | 229.7 (4.8%) |
| | 2 | 165.4 (0%) | 165.4 (0.3%) | 165.7 (0.9%) | 166.6 (1.9%) | 168.5 (3.1%) | 171.7 (4.3%) | 177.0 (5.5%) | 185.5 (6.3%) | 199.0 (6.0%) | 220.4 (4.2%) |
| | 3 | 165.4 (0%) | 165.4 (0.0%) | 165.5 (0.2%) | 165.7 (0.5%) | 166.6 (1.1%) | 168.4 (1.9%) | 171.9 (2.9%) | 178.5 (3.9%) | 190.5 (4.5%) | 212.6 (3.7%) |
| $m$=2 | 0 | 161.7 | 166.7 | 172.6 | 179.1 | 186.5 | 194.9 | 204.1 | 214.5 | 225.9 | 238.4 |
| | 1 | 161.7 (0%) | 162.1 (2.8%) | 163.6 (5.5%) | 166.3 (7.7%) | 170.1 (9.6%) | 175.7 (10.9%) | 183.4 (11.3%) | 193.9 (10.6%) | 208.2 (8.5%) | 227.2 (4.9%) |
| | 2 | 161.7 (0%) | 161.8 (0.2%) | 162.1 (0.9%) | 163.0 (2.0%) | 164.9 (3.2%) | 168.1 (4.5%) | 173.5 (5.7%) | 182.2 (6.5%) | 195.8 (6.3%) | 217.7 (4.4%) |
| | 3 | 161.7 (0%) | 161.7 (0.0%) | 161.8 (0.2%) | 162.1 (0.6%) | 162.9 (1.2%) | 164.8 (2.0%) | 168.4 (3.0%) | 175.1 (4.1%) | 187.3 (4.6%) | 209.9 (3.7%) |
| $m$=3 | 0 | 160.5 | 165.6 | 171.3 | 178.0 | 185.4 | 193.8 | 203.2 | 213.6 | 225.2 | 237.6 |
| | 1 | 160.5 (0%) | 160.9 (2.9%) | 162.4 (5.5%) | 165.1 (7.8%) | 168.9 (9.8%) | 174.6 (11.0%) | 182.3 (11.4%) | 192.9 (10.7%) | 207.3 (8.6%) | 226.3 (5.0%) |
| | 2 | 160.5 (0%) | 160.5 (0.3%) | 160.8 (1.0%) | 161.8 (2.0%) | 163.6 (3.3%) | 166.9 (4.6%) | 172.4 (5.8%) | 181.1 (6.6%) | 194.9 (6.3%) | 216.8 (4.4%) |
| | 3 | 160.5 (0%) | 160.5 (0.0%) | 160.5 (0.2%) | 160.8 (0.6%) | 161.7 (1.2%) | 163.5 (2.1%) | 167.1 (3.1%) | 173.9 (4.1%) | 186.2 (4.7%) | 208.9 (3.8%) |
| $m$=4 | 0 | 159.8 | 164.9 | 170.8 | 177.4 | 184.9 | 193.3 | 202.7 | 213.2 | 224.7 | 237.2 |
| | 1 | 159.8 (0%) | 160.3 (2.9%) | 161.8 (5.5%) | 164.4 (7.9%) | 168.3 (9.8%) | 174.0 (11.1%) | 181.8 (11.5%) | 192.5 (10.8%) | 206.8 (8.7%) | 225.8 (5.0%) |
| | 2 | 159.8 (0%) | 159.8 (0.3%) | 160.2 (1.0%) | 161.1 (2.0%) | 163.0 (3.3%) | 166.4 (4.6%) | 171.7 (5.8%) | 180.5 (6.6%) | 194.3 (6.4%) | 216.4 (4.4%) |
| | 3 | 159.8 (0%) | 159.8 (0.0%) | 159.9 (0.2%) | 160.2 (0.5%) | 161.0 (1.2%) | 162.9 (2.1%) | 166.6 (3.1%) | 173.3 (4.1%) | 185.6 (4.7%) | 208.5 (3.8%) |

**Table 9:** The steady-state *ARL*, *EARL* and *ARARL* of the (NSS, SSS, RSS, MSS) runs-rules and synthetic schemes with the 0&1 strategy (and 3&4 strategy – in brackets) when $\delta_{min}$= 0, $\delta_{max}$= 3, $\phi$=0.7, $\gamma$=0.7, $n \in \{3,10\}$ and $ARL_0$=370.4

| $n$ | $\delta$ | NSS: RR1,S1 | SSS: RR2,S2 | RSS: RR3,S3 | MSS: RR4,S4 |
|---|---|---|---|---|---|
| **3** | 0 | 370.4 (370.4) | 370.4 (370.4) | 370.4 (370.4) | 370.4 (370.4) |
| | 0.25 | 264.8 (206.8) | 217.2 (156.6) | 215.3 (154.7) | 201.4 (140.1) |
| | 0.5 | 124.7 (68.5) | 87.6 (47.7) | 86.3 (47.0) | 74.5 (39.0) |
| | 0.75 | 55.0 (25.1) | 38.7 (18.6) | 38.1 (18.4) | 31.2 (14.8) |
| | 1 | 26.6 (11.5) | 19.6 (9.2) | 19.4 (9.1) | 15.6 (7.5) |
| | 1.25 | 14.5 (6.5) | 11.4 (5.5) | 11.2 (5.5) | 9.1 (4.7) |
| | 1.5 | 8.9 (4.3) | 7.4 (3.9) | 7.3 (3.8) | 6.1 (3.4) |
| | 1.75 | 6.1 (3.2) | 5.2 (3.0) | 5.2 (3.0) | 4.4 (2.7) |
| | 2 | 4.5 (2.6) | 4.0 (2.5) | 4.0 (2.5) | 3.5 (2.4) |
| | 2.25 | 3.5 (2.3) | 3.3 (2.2) | 3.3 (2.2) | 3.0 (2.2) |
| | 2.5 | 3.0 (2.1) | 2.8 (2.1) | 2.8 (2.1) | 2.6 (2.1) |
| | 2.75 | 2.6 (2.0) | 2.5 (2.0) | 2.5 (2.0) | 2.4 (2.0) |
| | 3 | 2.3 (2.0) | 2.3 (2.0) | 2.3 (2.0) | 2.2 (2.0) |
| | ***EARL*** | 295.6 (235.8) | 257.5 (208.6) | 256.0 (207.6) | 242.1 (197.8) |
| | **%Diff** | 25.4% | 23.4% | 23.3% | 22.4% |
| | ***ARARL*** | 1.36 (1.26) | 1.14 (1.10) | 1.13 (1.09) | 1.00 (1.00) |
| **10** | 0 | 370.4 (370.4) | 370.4 (370.4) | 370.4 (370.4) | 370.4 (370.4) |
| | 0.25 | 200.4 (93.8) | 150.7 (65.2) | 148.8 (64.2) | 134.2 (54.3) |
| | 0.5 | 64.0 (17.3) | 44.7 (13.3) | 44.0 (13.2) | 36.4 (10.7) |
| | 0.75 | 23.1 (6.0) | 17.3 (5.2) | 17.1 (5.2) | 13.8 (4.4) |
| | 1 | 10.6 (3.3) | 8.6 (3.1) | 8.5 (3.1) | 7.0 (2.8) |
| | 1.25 | 6.0 (2.4) | 5.2 (2.3) | 5.2 (2.3) | 4.4 (2.2) |
| | 1.5 | 4.0 (2.1) | 3.7 (2.0) | 3.6 (2.0) | 3.2 (2.0) |
| | 1.75 | 3.0 (2.0) | 2.9 (2.0) | 2.9 (2.0) | 2.6 (2.0) |
| | 2 | 2.5 (2.0) | 2.4 (2.0) | 2.4 (2.0) | 2.3 (2.0) |
| | 2.25 | 2.2 (2.0) | 2.2 (2.0) | 2.2 (2.0) | 2.1 (2.0) |
| | 2.5 | 2.1 (2.0) | 2.0 (2.0) | 2.0 (2.0) | 2.0 (2.0) |
| | 2.75 | 2.0 (2.0) | 2.0 (2.0) | 2.0 (2.0) | 2.0 (2.0) |
| | 3 | 2.0 (2.0) | 2.0 (2.0) | 2.0 (2.0) | 2.0 (2.0) |
| | ***EARL*** | 230.8 (169.1) | 204.7 (157.8) | 203.7 (157.5) | 194.1 (152.9) |
| | **%Diff** | 36.5% | 29.7% | 29.4% | 26.9% |
| | ***ARARL*** | 1.26 (1.16) | 1.11 (1.06) | 1.10 (1.06) | 1.00 (1.00) |

**Table 10:** The yoghurt filling cup process dataset

| | | | | | | | | | | | **0&1** | **1&2** |
|---|---|---|---|---|---|---|---|---|---|---|---|---|
| | | $X_{t,1,1}$ | $X_{t,1,2}$ | $X_{t,2,1}$ | $X_{t,2,2}$ | $X_{t,3,1}$ | $X_{t,3,2}$ | $X_{t,4,1}$ | $X_{t,4,2}$ | $X_{t,5,1}$ | $X_{t,5,2}$ | $\bar{X}_t$ | $\bar{X}_t$ |
| | 1 | 124.9 | 124.8 | 125.9 | 125.9 | 125.2 | 124.8 | 124.6 | 124.1 | 124.8 | 124.4 | 125.33 | 124.82 |
| | 2 | 124.9 | 125.2 | 125.5 | 125.0 | 124.1 | 123.9 | 125.2 | 125.2 | 125.0 | 125.6 | 124.83 | 124.78 |
| | 3 | 125.1 | 125.1 | 125.2 | 124.8 | 125.4 | 125.3 | 122.9 | 122.4 | 125.4 | 125.4 | 125.23 | 125.28 |
| | 4 | 126.1 | 125.9 | 124.6 | 124.8 | 125.7 | 125.5 | 126.4 | 126.5 | 124.9 | 125.7 | 125.47 | 125.63 |
| | 5 | 125.8 | 125.7 | 122.6 | 122.6 | 124.1 | 123.5 | 126.1 | 126.3 | 124.9 | 125.0 | 124.17 | 124.83 |
| | 6 | 125.0 | 125.2 | 125.5 | 124.8 | 124.8 | 125.0 | 124.9 | 124.8 | 124.8 | 124.2 | 125.10 | 124.83 |
| | 7 | 124.2 | 124.6 | 125.8 | 125.3 | 125.4 | 125.5 | 126.4 | 126.2 | 125.1 | 125.2 | 125.13 | 125.00 |
| | 8 | 124.9 | 124.9 | 123.8 | 123.2 | 125.1 | 125.3 | 124.0 | 124.5 | 124.4 | 124.2 | 124.60 | 124.80 |
| $t$ | 9 | 125.9 | 125.8 | 124.4 | 124.8 | 126.3 | 125.7 | 124.9 | 125.2 | 125.2 | 125.1 | 125.53 | 125.67 |
| | 10 | 124.2 | 124.3 | 126.2 | 125.5 | 125.6 | 125.0 | 124.4 | 124.4 | 124.1 | 124.3 | 125.33 | 124.58 |
| | 11 | 123.7 | 123.6 | 123.4 | 123.3 | 124.7 | 124.8 | 123.1 | 123.1 | 123.1 | 122.8 | 123.93 | 123.78 |
| | 12 | 124.0 | 124.1 | 122.6 | 122.4 | 123.6 | 123.6 | 124.4 | 124.5 | 123.6 | 123.1 | 123.40 | 123.67 |
| | 13 | 122.0 | 122.5 | 123.9 | 124.0 | 123.7 | 124.1 | 124.3 | 124.4 | 121.9 | 122.9 | 123.20 | 122.85 |
| | 14 | 122.4 | 123.0 | 122.8 | 123.1 | 123.7 | 124.2 | 123.7 | 124.1 | 122.8 | 123.1 | 122.97 | 123.20 |
| | 15 | 123.9 | 123.6 | 124.1 | 124.5 | 123.4 | 122.9 | 123.1 | 123.1 | 124.5 | 125.1 | 123.80 | 123.90 |
| | 16 | 121.9 | 122.3 | 123.4 | 123.3 | 123.5 | 123.3 | 125.3 | 125.5 | 123.3 | 123.6 | 122.93 | 122.98 |
| | 17 | 123.3 | 122.9 | 123.6 | 123.5 | 124.2 | 123.8 | 123.4 | 123.6 | 123.5 | 123.4 | 123.70 | 123.52 |
| | 18 | 122.0 | 122.2 | 123.6 | 123.4 | 124.7 | 125.0 | 122.6 | 122.5 | 124.5 | 123.9 | 123.43 | 123.72 |
| | 19 | 124.0 | 123.9 | 123.1 | 123.4 | 123.9 | 124.5 | 122.6 | 122.8 | 124.2 | 123.5 | 123.67 | 124.00 |
| | 20 | 125.5 | 124.9 | 122.2 | 122.3 | 123.2 | 123.2 | 123.2 | 123.3 | 123.2 | 123.2 | 123.63 | 123.87 |

**Table 11:** The RR4 or S4 *s&m* scheme using the yoghurt filling cup example in steady-state mode when $\gamma$=0.316, $\phi$=0.38, $H$=1, $n$=3, $m\in\{1,2\}$ and $s\in\{0,1\}$

| | $s$ | 0 | 1 |
|---|---|---|---|
| | $m$ | 1 | 2 |
| | $C_1(m,\gamma)$ | 0.9536 | 0.9760 |
| | $C_2(n,\phi,s)$ | 0.7898 | 0.9104 |
| | $C_3(m,n,\gamma,\phi,s)$ | 0.7664 | 0.8922 |
| RR4 or S4 | $UCL$ | 125.92 | 125.78 |
| | $LCL$ | 123.88 | 124.02 |
| $\bar{X}$ | $UCL$ | 126.62 | 126.38 |
| | $LCL$ | 123.18 | 123.43 |